

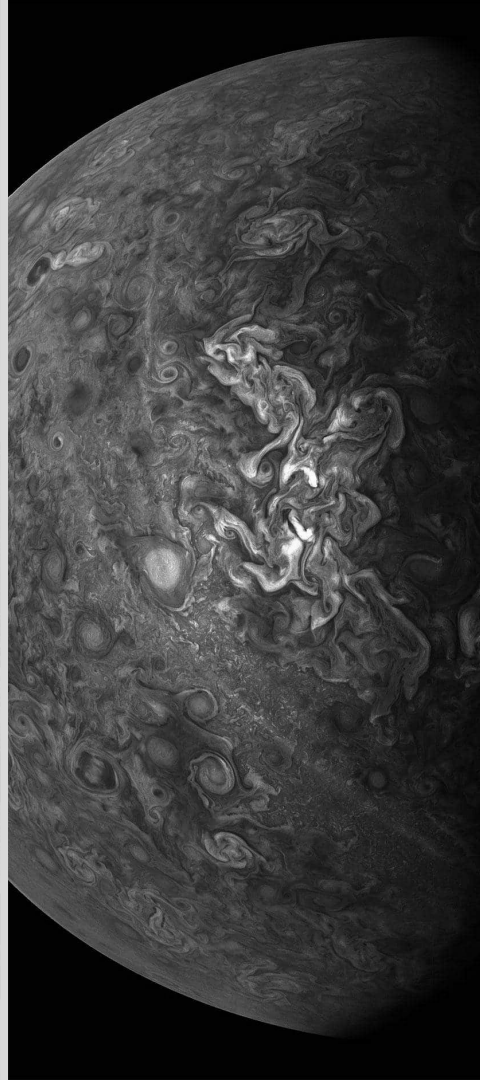
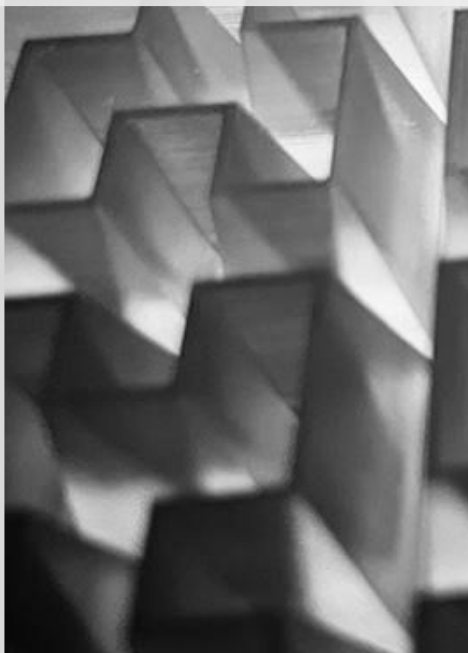
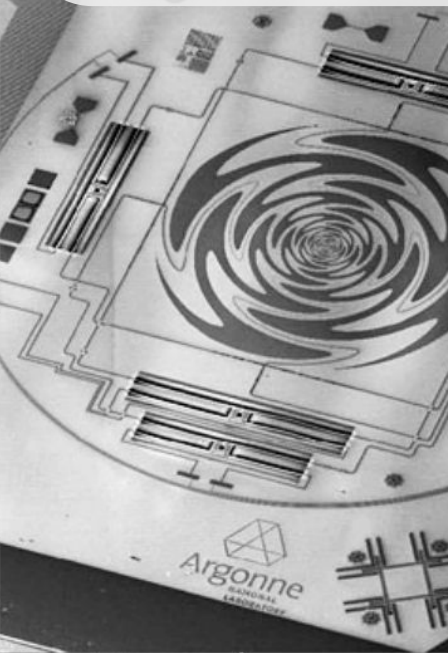
# Knowing your beams

Jon E. Gudmundsson

Stockholm University and the Oskar Klein Centre

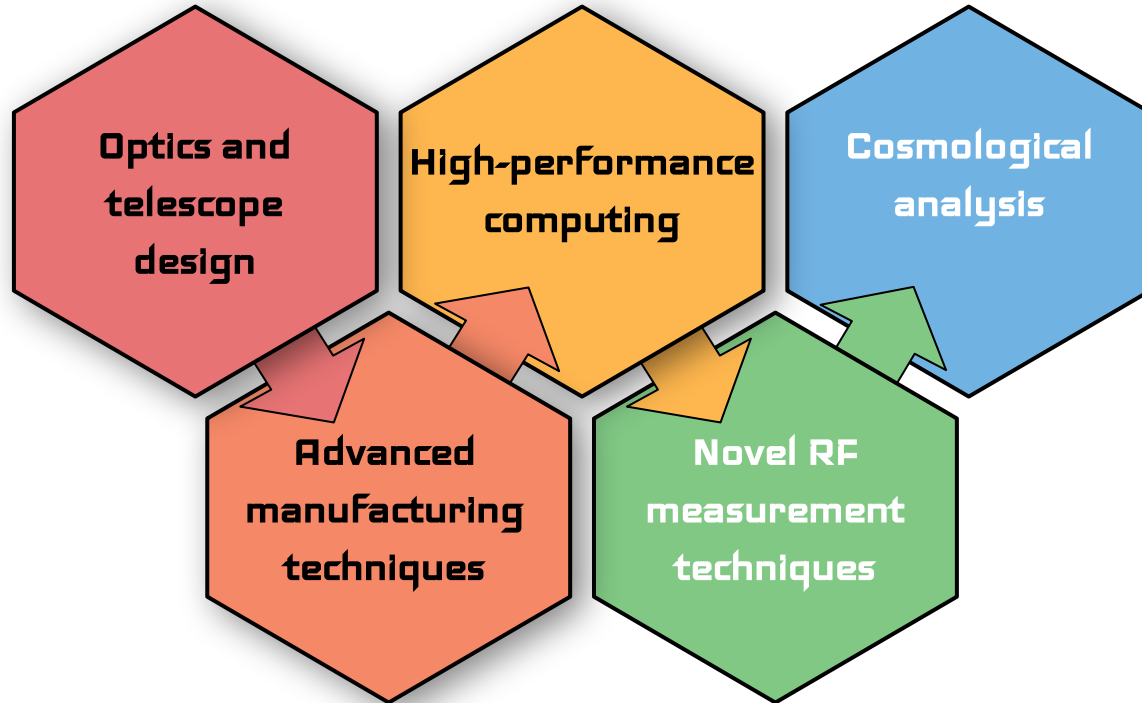
*From Planck to the future of CMB*

*Ferrara, May 2022*



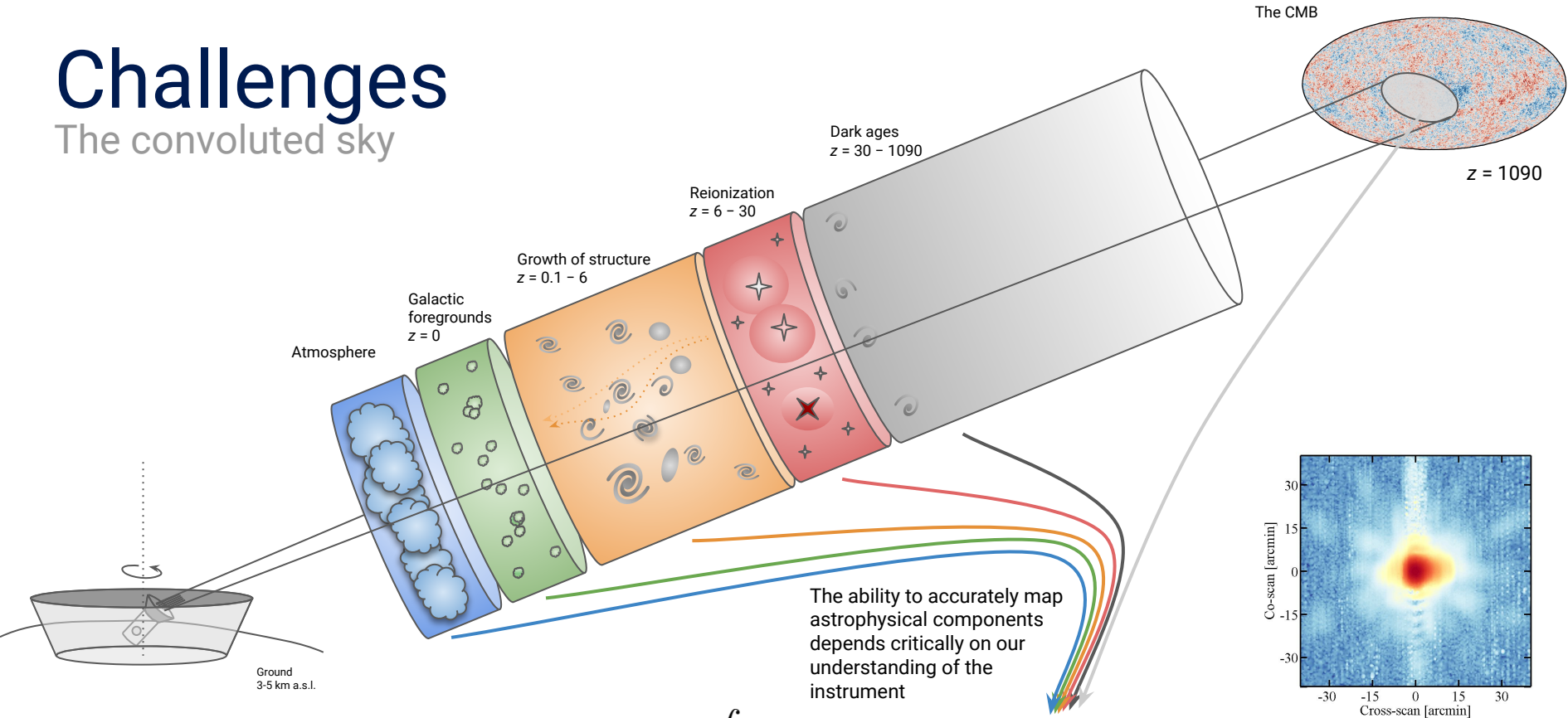
# Knowing your beams implies...

...GRASPIng a number of concepts

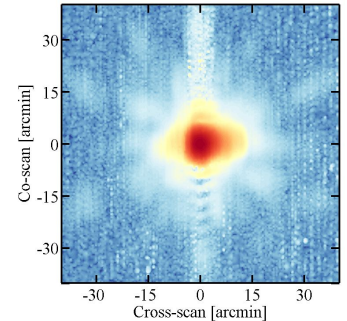


# Challenges

The convoluted sky

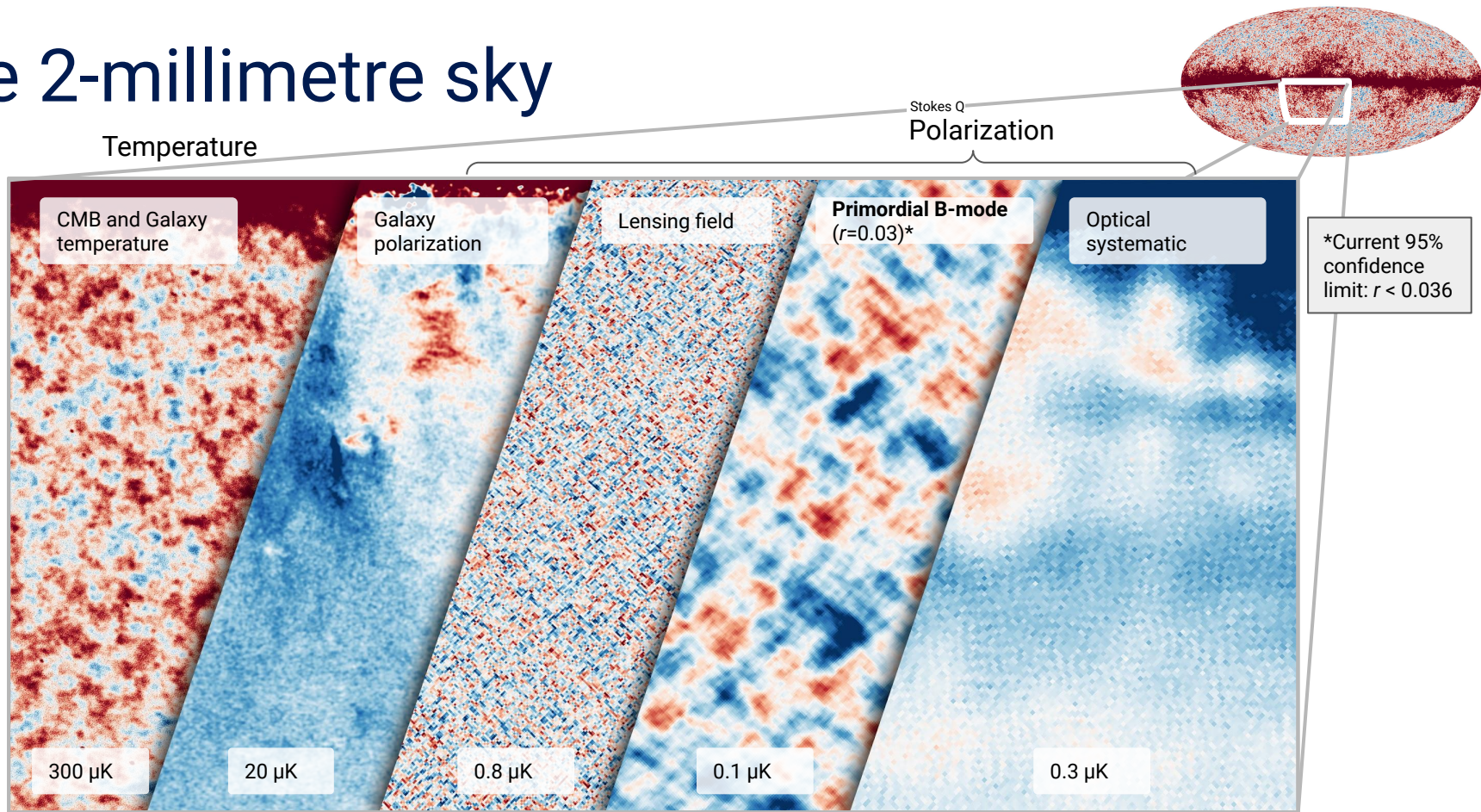


$$\text{signal} \propto \int \underbrace{B(\theta - \theta_0, \phi - \phi_0)}_{\text{Beam}} \underbrace{P(\theta, \phi)}_{\text{Power}} d\Omega$$



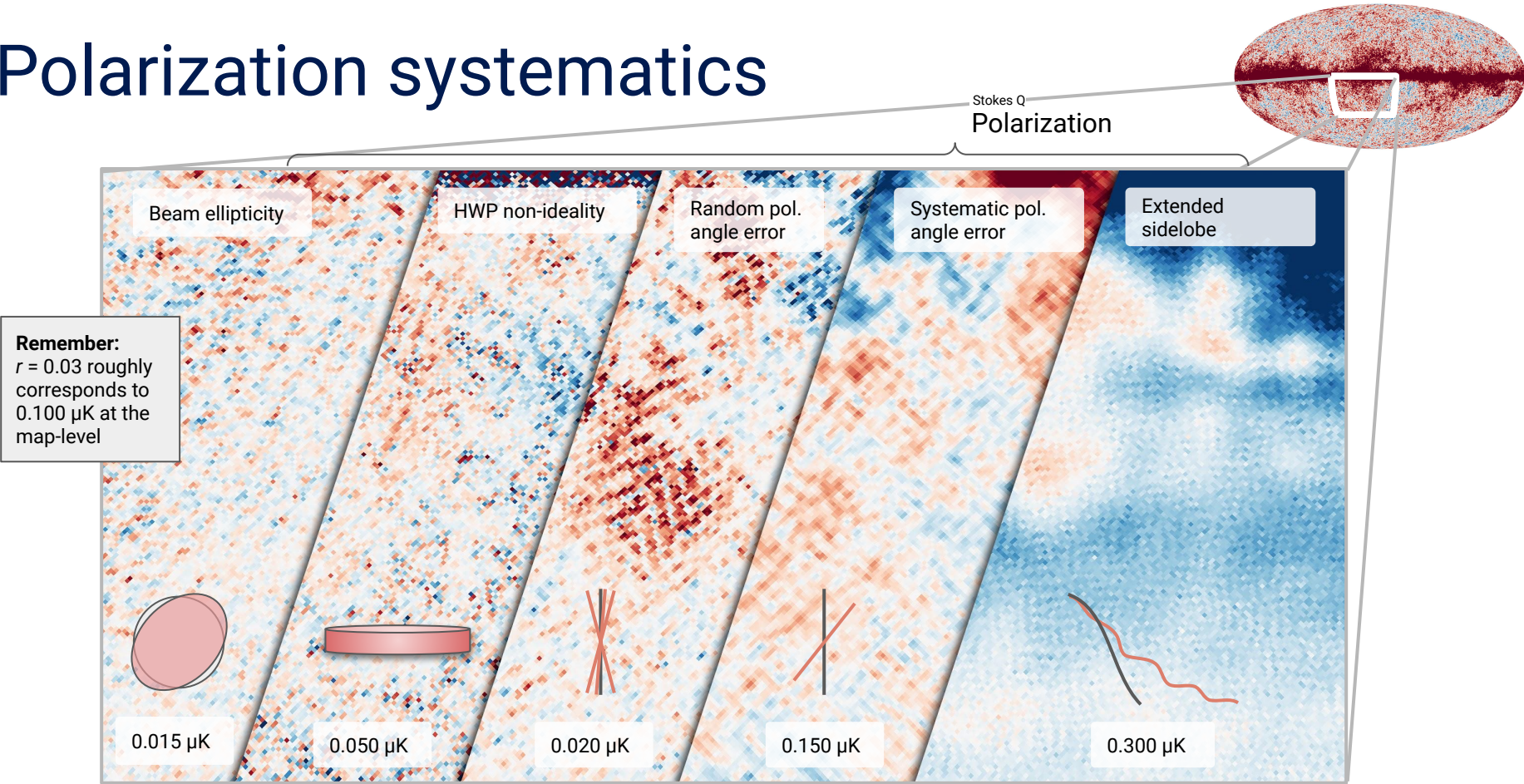
Example beam,  $B(\theta, \phi)$ , for a Planck detector at 545 GHz  
Planck 2015 results. VII. A&A (2016)

# The 2-millimetre sky



Full panel covers a roughly  $80 \times 35^\circ$  region on the sky with the Galactic plane near the top  
Simulations generated with beamconv, see [Duivenvoorden et al., MNRAS \(2018 and 2021\)](https://arxiv.org/abs/1805.03421)  
<https://github.com/AdriJD/beamconv>

# Polarization systematics



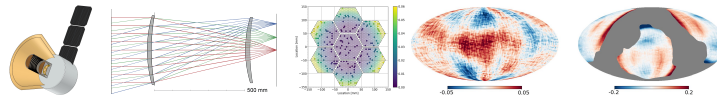
Full panel covers a roughly  $80 \times 35^\circ$  region on the sky with the Galactic plane near the top  
Simulations generated with beamconv, see **Duivenvoorden et al.**, *MNRAS* (2018 and 2021)  
<https://github.com/AdriJD/beamconv>

# Outline

- **Forward modeling of optical systematics**
  - Understanding what is and what isn't important
- **Calibration of CMB instruments**
  - What have we learned? Where can we improve?
- **Optical modeling**
  - Where do our modeling capabilities fall short and what can we do about it?

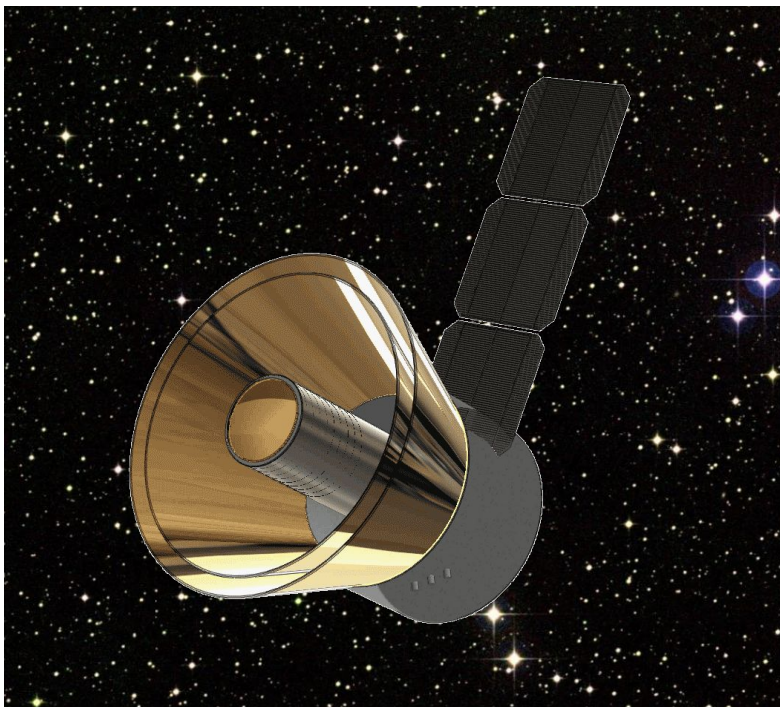
# *beamconv* published in 2018

- Open source spherical harmonic beam convolution algorithm **written in Python**
  - <https://github.com/AdriJD/beamconv>
- Spin-spherical harmonic representations of the (polarized) beam response and sky to generate simulated CMB detector signal timelines
- **Beams can be arbitrarily shaped; pointing timelines can be read in or calculated on the fly**; optionally, the results can be binned on the sphere
- First paper: Duivenvoorden, JEG, and Rahlin, MNRAS (2019) ([arXiv:1809.05034](https://arxiv.org/abs/1809.05034))
  - Core algorithm first described in Prézeau and Reinecke, ApJS, 190:267–274 (2010)



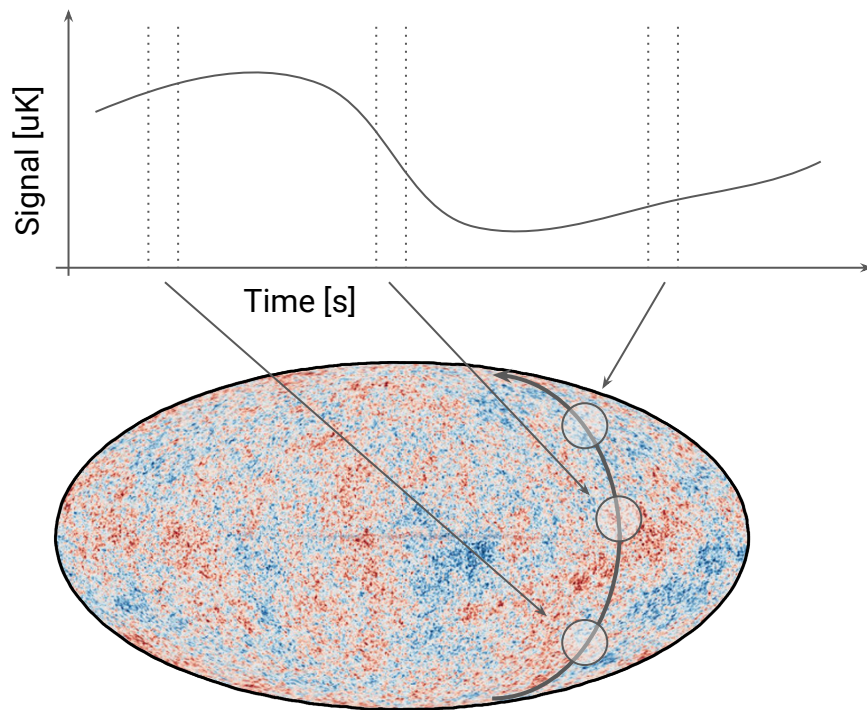
A. Duivenvoorden  
Stockholm  
University '19

# Scanning the sky



Fiducial satellite, adapted from Duivenvoorden et al. (2018)

$$\text{signal} \propto \int \underbrace{B(\theta - \theta_0, \phi - \phi_0)}_{\text{Beam}} \underbrace{P(\theta, \phi)}_{\text{Power}} d\Omega$$



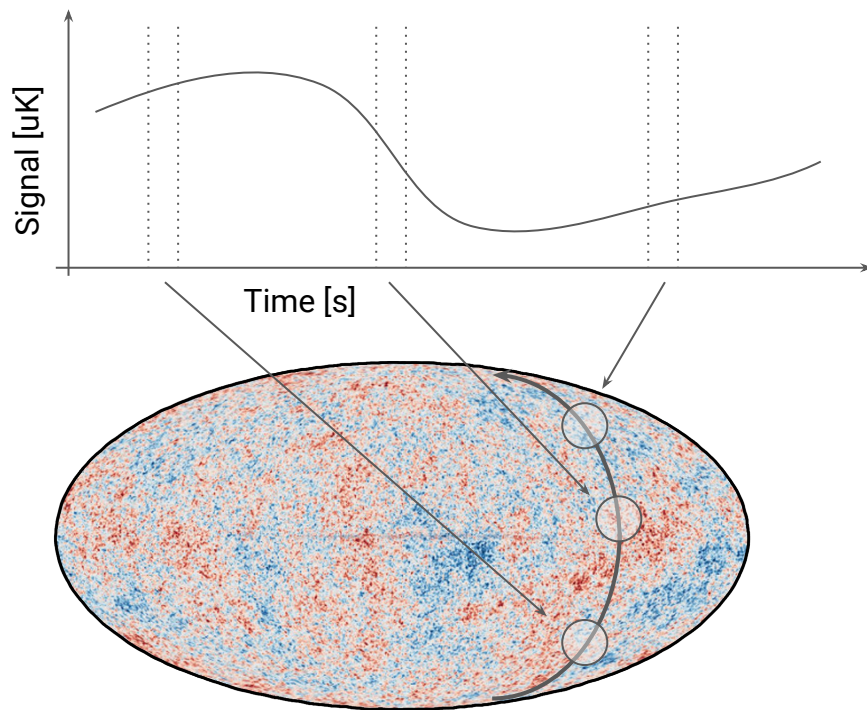


# Beam convolution simple for symmetric beams

Time-ordered data modelled as:

$$d_t = \sum_{\ell m} \underbrace{B_\ell}_{\text{blue}} \underbrace{a_{\ell m}}_{\text{purple}} \underbrace{Y_{\ell m}(\hat{\mathbf{n}}_t)}_{\text{orange}}$$

- $B_\ell$  : Legendre coefficients beam
- $a_{\ell m}$  : harmonic modes of sky
- $Y_{\ell m}(\hat{\mathbf{n}}_t)$  : spherical harmonic evaluated at beam center

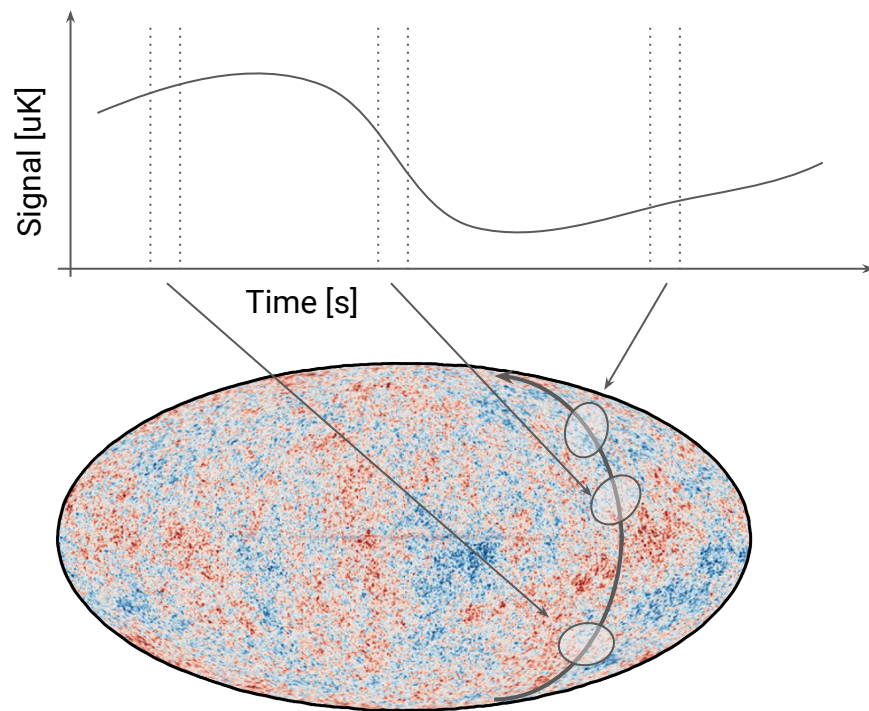


# Asymmetric beam complicates matters

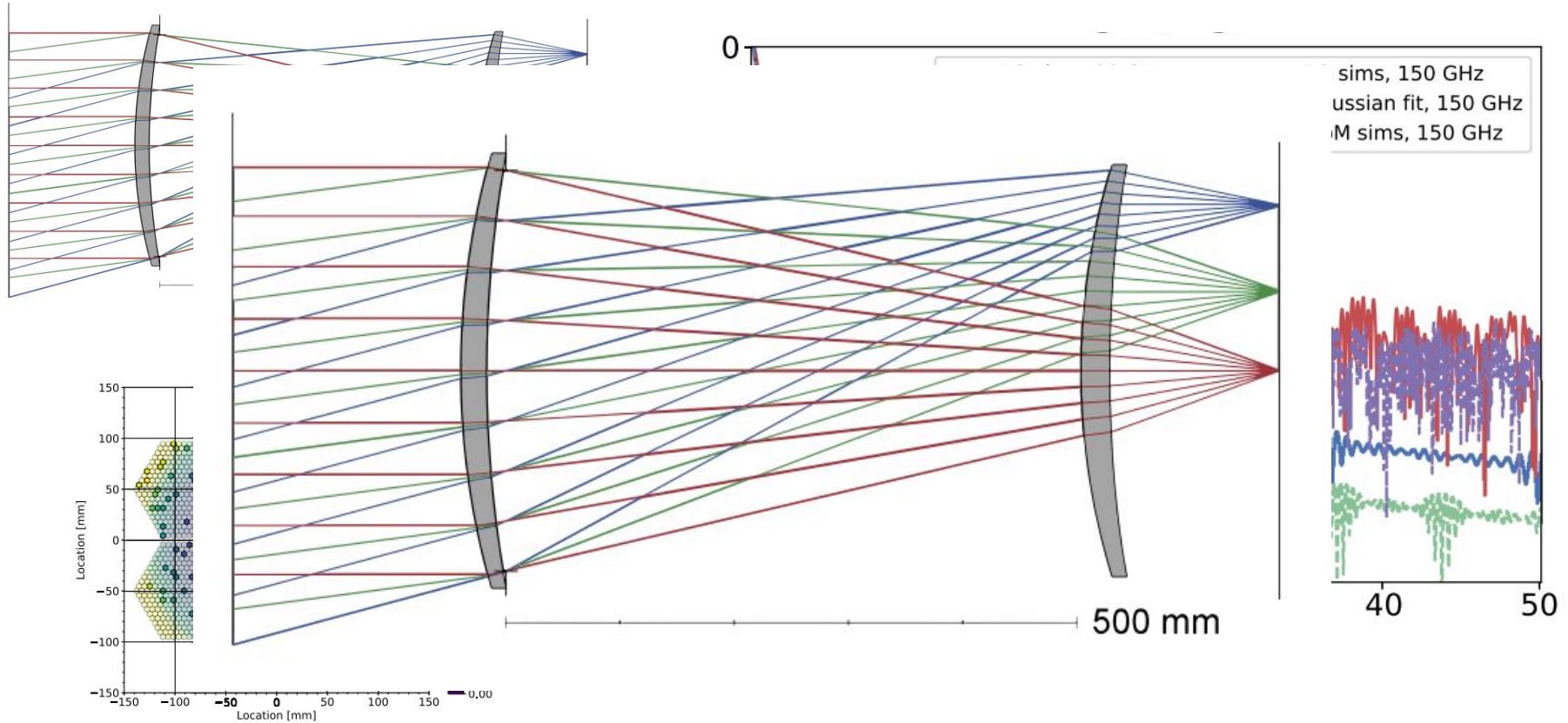
Time-ordered data modelled as:

$$d_t = \sum_s \left[ \sum_{lm} \underbrace{B_{\ell s}}_{\text{blue}} \underbrace{a_{\ell m}}_{\text{purple}} \underbrace{{}_s Y_{\ell m}(\hat{\mathbf{n}}_t)}_{\text{orange}} \right] e^{-is\psi_t}$$

- $B_{\ell s}$  : harmonic modes of beam
- $a_{\ell m}$  : harmonic modes of sky
- ${}_s Y_{\ell m}(\hat{\mathbf{n}}_t)$  : spin-weighted spherical harmonic evaluated at beam center
- $e^{-is\psi_t}$  : orientation of detector with respect to sky

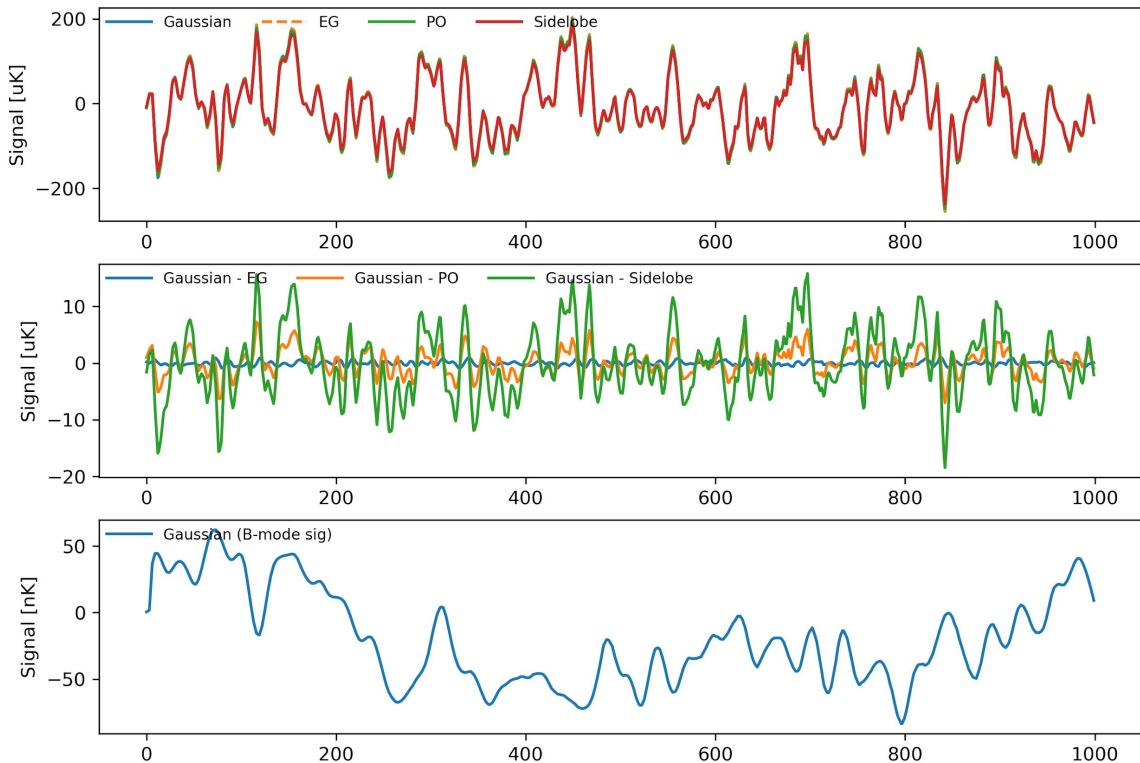
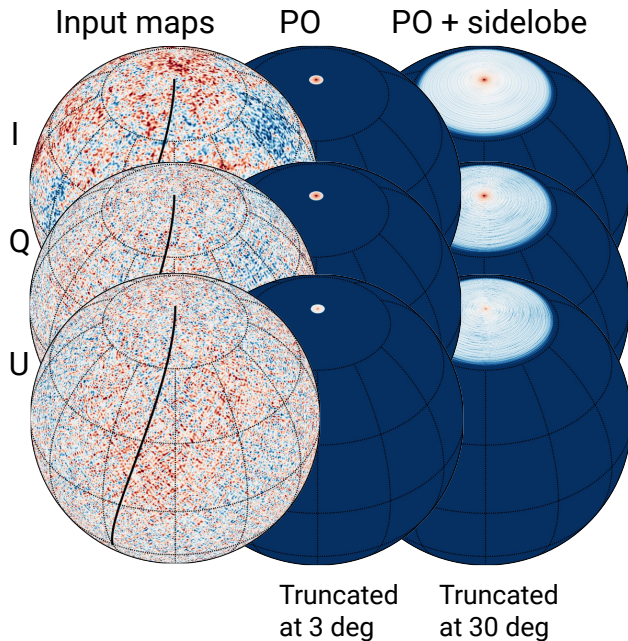


# Two-lens refractor design

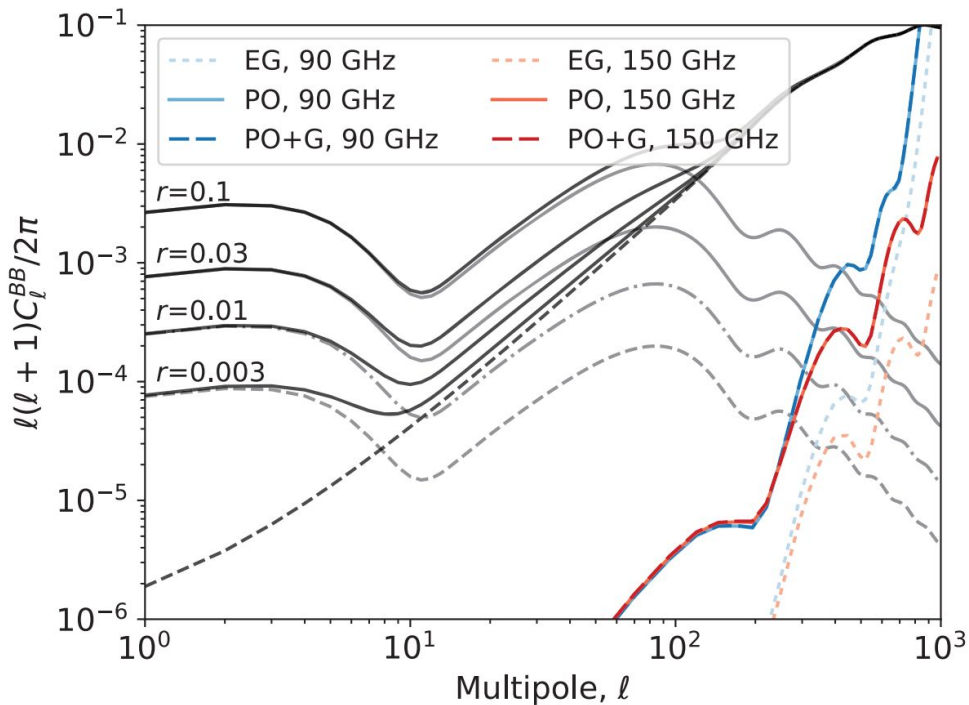
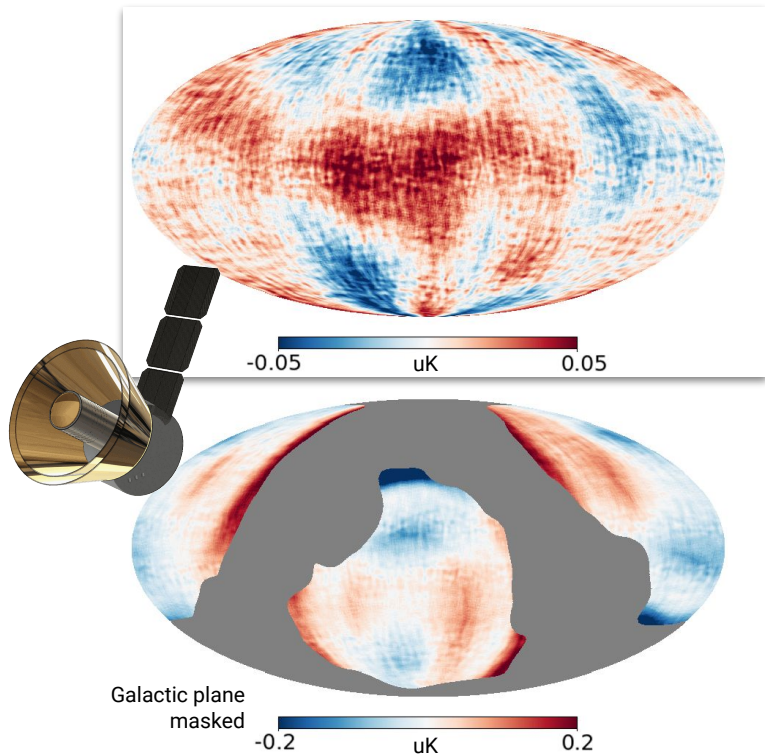


# Time-domain simulation example

Scanning the sky with a 19-arcmin FWHM beam and gradually increasing model complexity

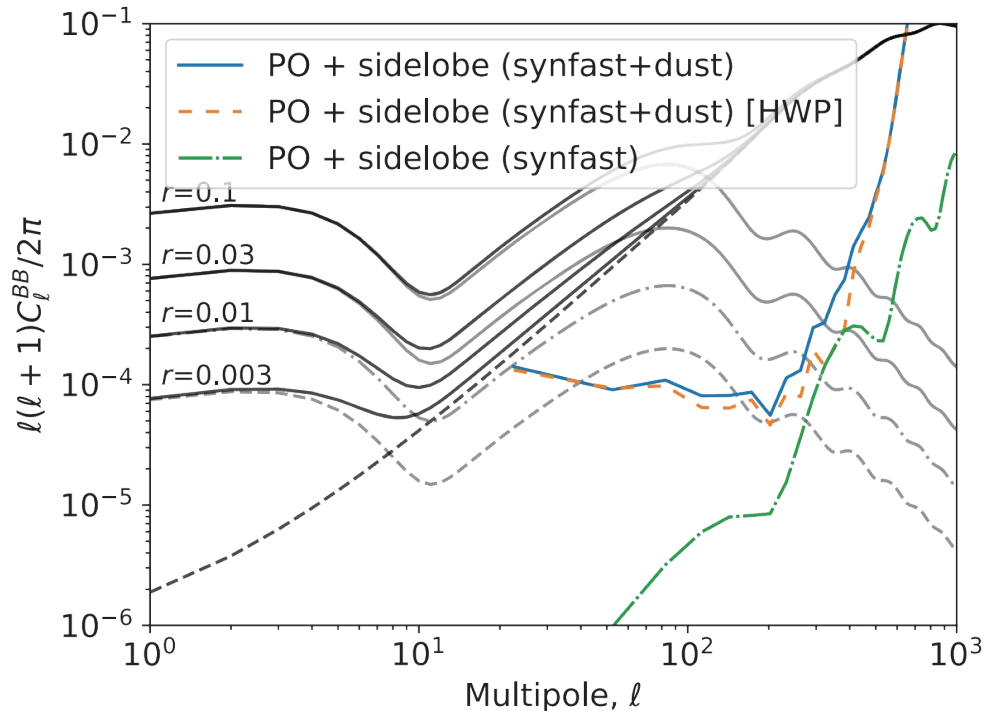
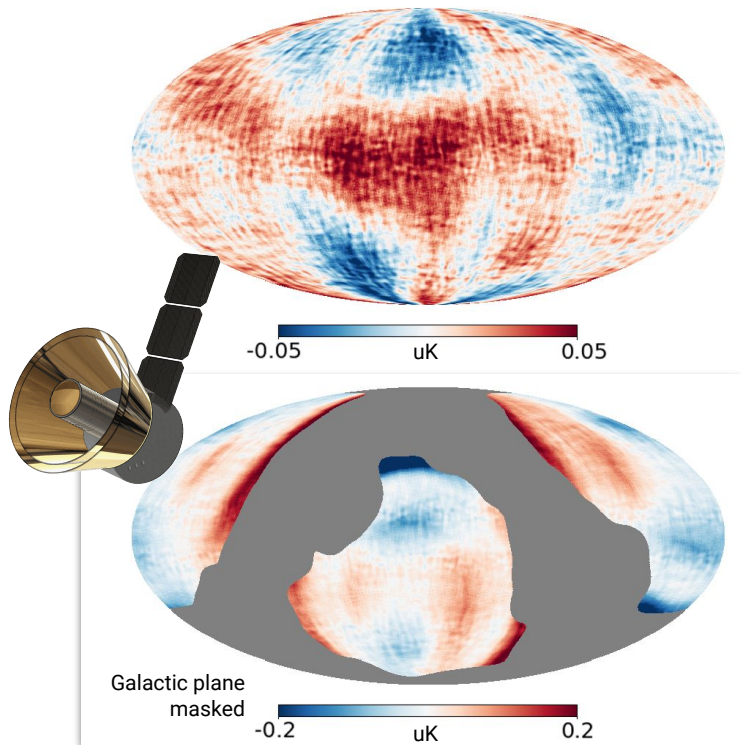


# beamconv results



[Duivenvoorden, JEG, and Rahlin, MNRAS \(2019\) \(arXiv:1809.05034\)](#)

# beamconv results



**Key result:** Realistic beam sidelobe models will couple to polarized Galactic foregrounds in a way that can be quite problematic for future instruments

[Duivenvoorden, JEG, and Rahlin, MNRAS \(2018\) \(arXiv:1809.05034\)](#)

# beamconv with polarization modulators

Monthly Notices

of the  
ROYAL ASTRONOMICAL SOCIETY

MNRAS **502**, 4526–4539 (2021)

Advance Access publication 2021 February 6



doi:10.1093/mnras/stab317

## Probing frequency-dependent half-wave plate systematics for CMB experiments with full-sky beam convolution simulations

Adriaan J. Duivenvoorden<sup>1</sup>,<sup>1\*</sup> Alexandre E. Adler,<sup>2</sup> Matteo Billi,<sup>3,4,5</sup> Nadia Dachlythra<sup>2</sup> and Jon E. Gudmundsson<sup>2</sup>

<sup>1</sup>Joseph Henry Laboratories of Physics, Jadwin Hall, Princeton University, Princeton, NJ 08544, USA

<sup>2</sup>The Oskar Klein Centre, Department of Physics, Stockholm University, AlbaNova, SE-10691 Stockholm, Sweden

<sup>3</sup>Dipartimento di Fisica e Astronomia, Alma Mater Studiorum Università di Bologna, Via Gobetti 93/2, I-40129 Bologna, Italy

<sup>4</sup>INAF–OAS Bologna, Osservatorio di Astrofisica e Scienza dello Spazio di Bologna, Istituto Nazionale di Astrofisica, via Gobetti 101, I-40129 Bologna, Italy

<sup>5</sup>Istituto Nazionale di Fisica Nucleare (INFN), Sezione di Bologna, viale Bert Pichat 6/2, I-40127 Bologna, Italy

Accepted 2021 January 27. in original form 2021 January 20

### ABSTRACT

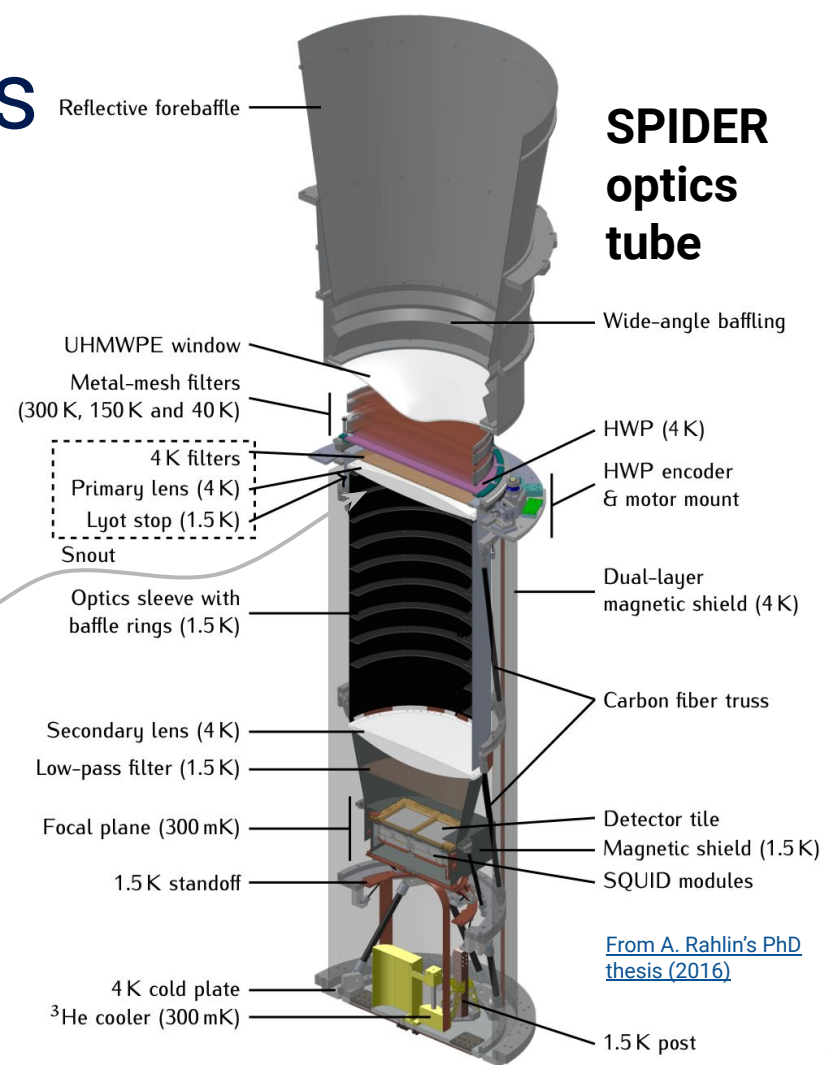
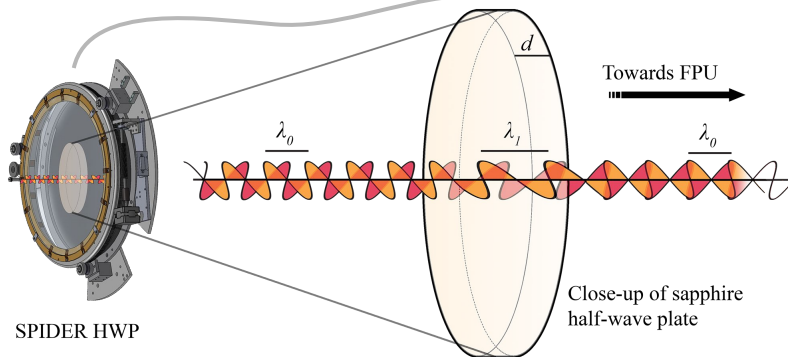
We study systematic effects from half-wave plates (HWP) for cosmic microwave background (CMB) experiments using full-sky time-domain beam convolution simulations. Using an optical model for a fiducial spaceborne two-lens refractor telescope, we investigate how different HWP configurations optimized for dichroic detectors centred at 95 and 150 GHz impact the reconstruction of primordial B-mode polarization. We pay particular attention to possible biases arising from the interaction of frequency-dependent HWP non-idealities with polarized Galactic dust emission and the interaction between the HWP and the instrumental beam. To produce these simulations, we have extended the capabilities of the publicly available BEAMCONV code. To our knowledge, we produce the first time-domain simulations that include both HWP non-idealities and realistic full-sky beam convolution. Our analysis shows how certain achromatic HWP configurations produce significant systematic polarization angle offsets that vary for sky components with different frequency dependence. Our analysis also demonstrates that once we account for interactions with HWPs, realistic beam models with non-negligible cross-polarization and sidelobes will cause significant B-mode residuals that will have to be extensively modelled in some cases.

**Key words:** polarization – methods: numerical – techniques: polarimetric – telescopes – cosmic background radiation – cosmology; observations.

- First time that we capture complex interplay between the **polarized** far field beam response and polarization modulators (HWPs)
- This functionality should be folded into future simulation infrastructure, i.e. Toast and the LiteBIRD Simulation Framework

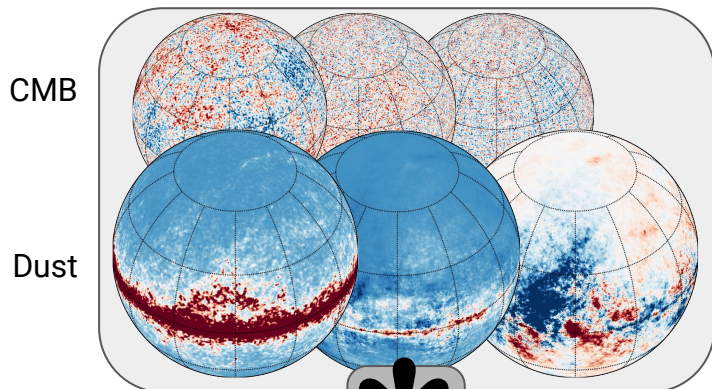
# Polarization modulators

- Used to **improve cross-linking** and **modulate polarized signal** relative to unpolarized light (suppress low-frequency noise)
- Most common type are birefringent **sapphire plates**, but wire grids and metamaterial modulators also being developed
- Sapphire cut to correct thickness is a half-wave plate
- High-index ( $n \sim 3$ ) sapphire must include anti-reflection coating
  - Broadband coverage challenging
  - Particularly relevant for future satellite missions such as LiteBIRD
  - Metamaterial and VPMs suffer also suffer from similar non-idealities





# beamconv cont.



A. Duivenvoorden  
SU '19



A. Adler  
SU '23

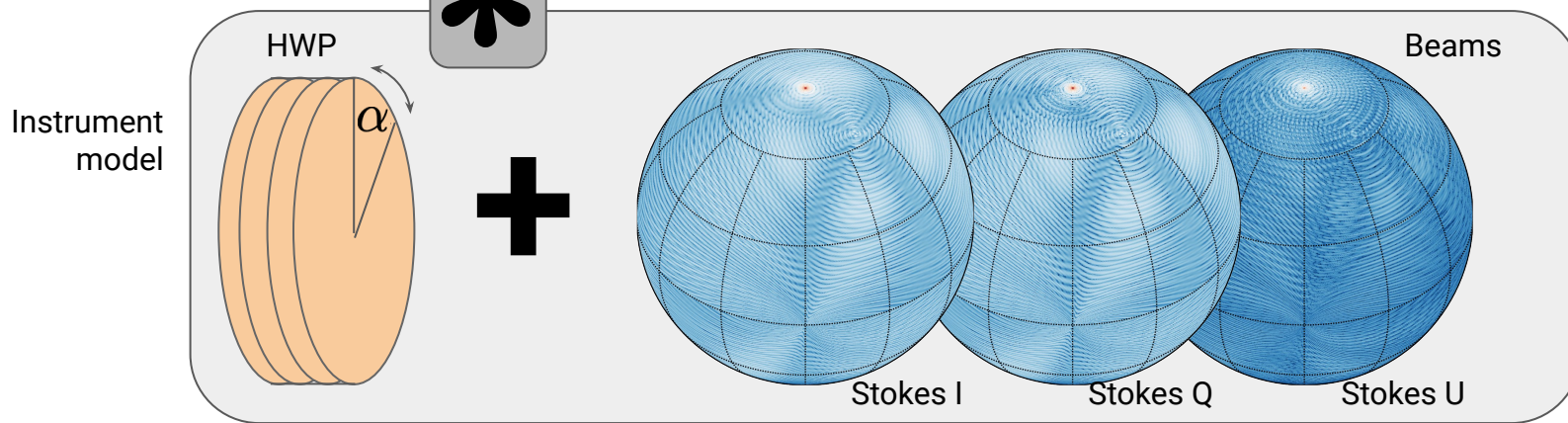


N. Dachlythra  
SU '23



M. Billi  
U. Bologna '22

<https://github.com/AdriJD/beamconv>  
[Duivenvoorden, JEG, & Rahlin, MNRAS \(2018\)](#)  
[Duivenvoorden et al., MNRAS \(2021\)](#)



# Data model

Data model as the inner product of a Stokes vector representing the instrumental response and a rotated stokes vector of the sky

$$d_t = S_{\text{instrument}} M_{\text{rot},t} S_{\text{sky}}$$

$$d_t = \sum_s \left[ \sum_{lm} B_{\ell s} a_{\ell m s} Y_{\ell m}(\hat{\mathbf{n}}_t) \right] e^{-is\psi_t}$$

# Frequency-independent data model

$$\begin{aligned}
 d_t = \sum_s \sum_{\ell, m} \left\{ B_{\ell s}^{\tilde{I}_i^{(0)}}(\alpha_t) a_{\ell m}^I + B_{\ell s}^{\tilde{V}_i^{(0)}}(\alpha_t) a_{\ell m}^V \right. \\
 \left. + \frac{1}{2} \left[ -2 B_{\ell s}^{\tilde{P}_i^{(0)}}(\alpha_t) 2 a_{\ell m}^P + 2 B_{\ell s}^{\tilde{P}_i^{(0)}}(\alpha_t) -2 a_{\ell m}^P \right] \right\} \\
 \times {}_s Y_{\ell m}(\hat{\mathbf{n}}_t) e^{-is\psi_t}
 \end{aligned}$$

Coupling to **Stokes I** of sky described by (note the  $2\alpha$  terms):

$$\begin{aligned}
 B_{\ell s}^{\tilde{I}_i^{(0)}}(\alpha_t) = B_{\ell s}^{\tilde{I}_b, II} + B_{\ell s}^{\tilde{V}_b, VI} \\
 + B_{\ell s}^{\text{Re}(\tilde{P}_b, P^* I)} \cos(2\alpha_t) + B_{\ell s}^{\text{Im}(\tilde{P}_b, P^* I)} \sin(2\alpha_t)
 \end{aligned}$$

# Frequency-independent data model

$$\begin{aligned}
 d_t = \sum_s \sum_{\ell, m} \left\{ B_{\ell s}^{\tilde{I}_i^{(0)}}(\alpha_t) a_{\ell m}^I + B_{\ell s}^{\tilde{V}_i^{(0)}}(\alpha_t) a_{\ell m}^V \right. \\
 \left. + \frac{1}{2} \left[ -2 B_{\ell s}^{\tilde{P}_i^{(0)}}(\alpha_t) 2 a_{\ell m}^P + 2 B_{\ell s}^{\tilde{P}_i^{(0)}}(\alpha_t) -2 a_{\ell m}^P \right] \right\} \\
 \times {}_s Y_{\ell m}(\hat{\mathbf{n}}_t) e^{-is\psi_t}
 \end{aligned}$$

Coupling to **Stokes V** of sky described by (note the  $2\alpha$  terms):

$$\begin{aligned}
 B_{\ell s}^{\tilde{V}_i^{(0)}}(\alpha_t) = B_{\ell s}^{\tilde{I}_b, IV} + B_{\ell s}^{\tilde{V}_b, VV} \\
 + B_{\ell s}^{\text{Re}(\tilde{P}_b, P^* V)} \cos(2\alpha_t) + B_{\ell s}^{\text{Im}(\tilde{P}_b, P^* V)} \sin(2\alpha_t)
 \end{aligned}$$

# Frequency-independent data model

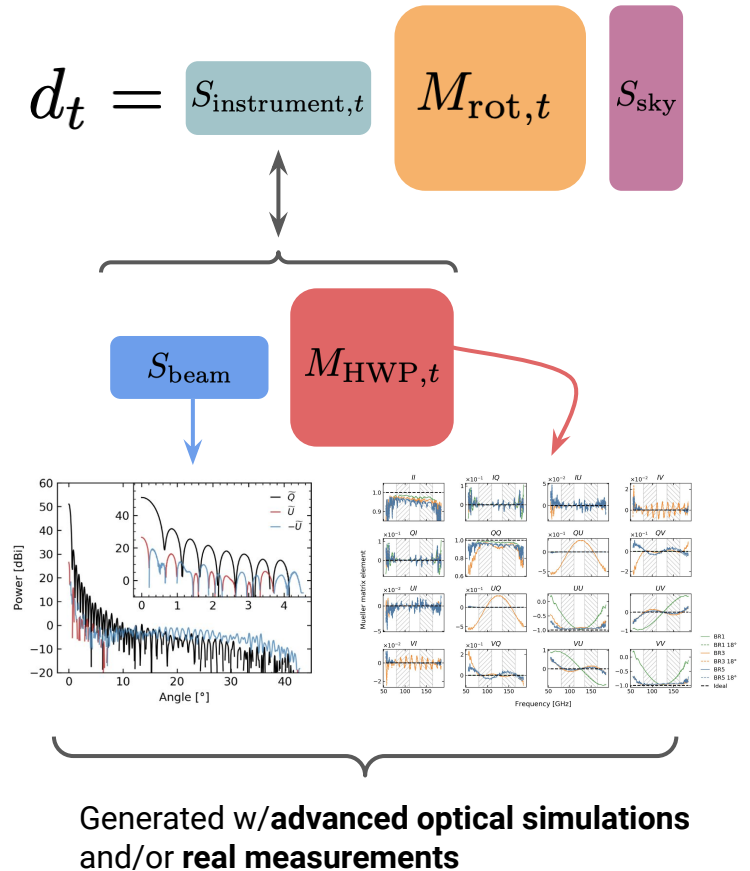
$$\begin{aligned}
 d_t = & \sum_s \sum_{\ell, m} \left\{ B_{\ell s}^{\tilde{I}_i^{(0)}}(\alpha_t) a_{\ell m}^I + B_{\ell s}^{\tilde{V}_i^{(0)}}(\alpha_t) a_{\ell m}^V \right. \\
 & + \frac{1}{2} \left[ \boxed{-2B_{\ell s}^{\tilde{P}_i^{(0)}}(\alpha_t)} 2a_{\ell m}^P + \boxed{2B_{\ell s}^{\tilde{P}_i^{(0)}}(\alpha_t)} -2a_{\ell m}^P \right] \left. \right\} \\
 & \times {}_s Y_{\ell m}(\hat{\mathbf{n}}_t) e^{-is\psi_t}
 \end{aligned}$$

Coupling to **Stokes Q/U** of sky described by (note the  $2\alpha$  and  $0\alpha$  terms):

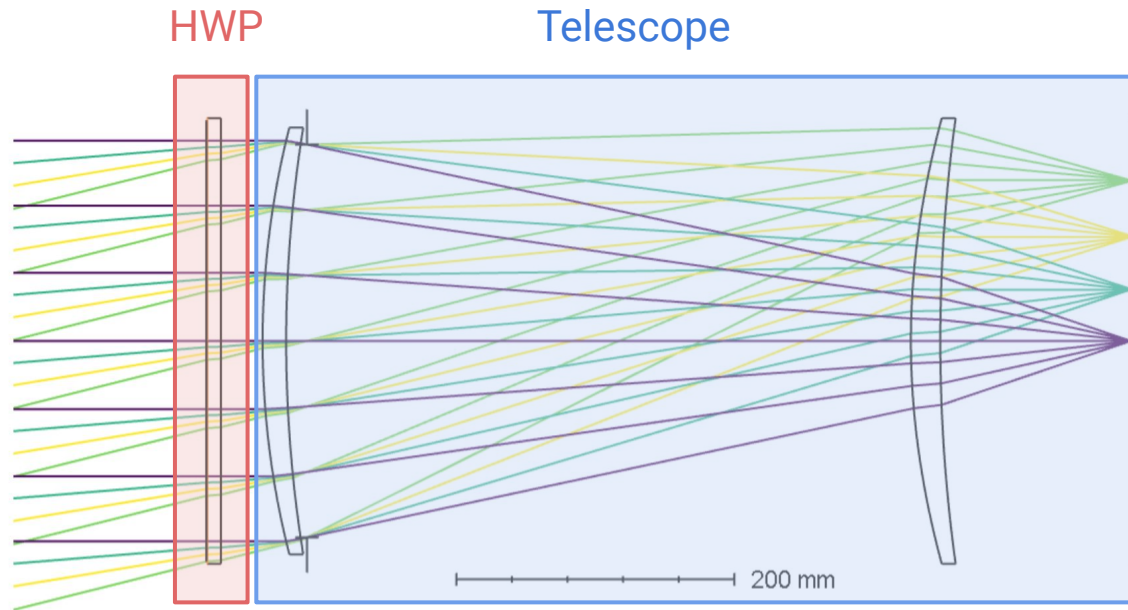
$$\begin{aligned}
 \boxed{{}_2 B_{\ell s}^{\tilde{P}_i^{(0)}}(\alpha_t)} = & {}_2 B_{\ell s}^{\tilde{I}_b, IP} e^{-2i\alpha t} + {}_2 B_{\ell s}^{\tilde{V}_b, VP} e^{-2i\alpha t} \\
 & + {}_2 B_{\ell s}^{\tilde{P}_b^*, P^* P} e^{-4i\alpha t} + {}_2 B_{\ell s}^{\tilde{P}_b, PP}
 \end{aligned}$$

# The approximation

- The instrumental Stokes vector can be factored into a Stokes vector describing the beam response and a Mueller matrix describing the skywards HWP
- Strictly speaking, the factorization of the beam and HWP is only valid if the radiation field between the HWP and beam-forming elements (lenses) can be described **by a plane wave parallel to the principal ray of the optics**
- The interaction between the near-field beam and the HWP will in reality also be sensitive to the longitudinal component of the electric field in between the optical elements, but accounting for these near-field effects beyond the scope of this work

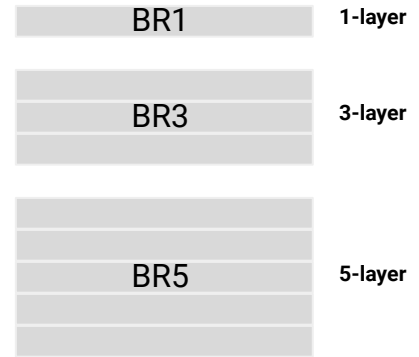


# Instrument model



## Half-wave plates

Broadband (achromatic) polarization modulators obtained by stacking birefringent plates



The HWP defines the Mueller matrix that acts on the far field response

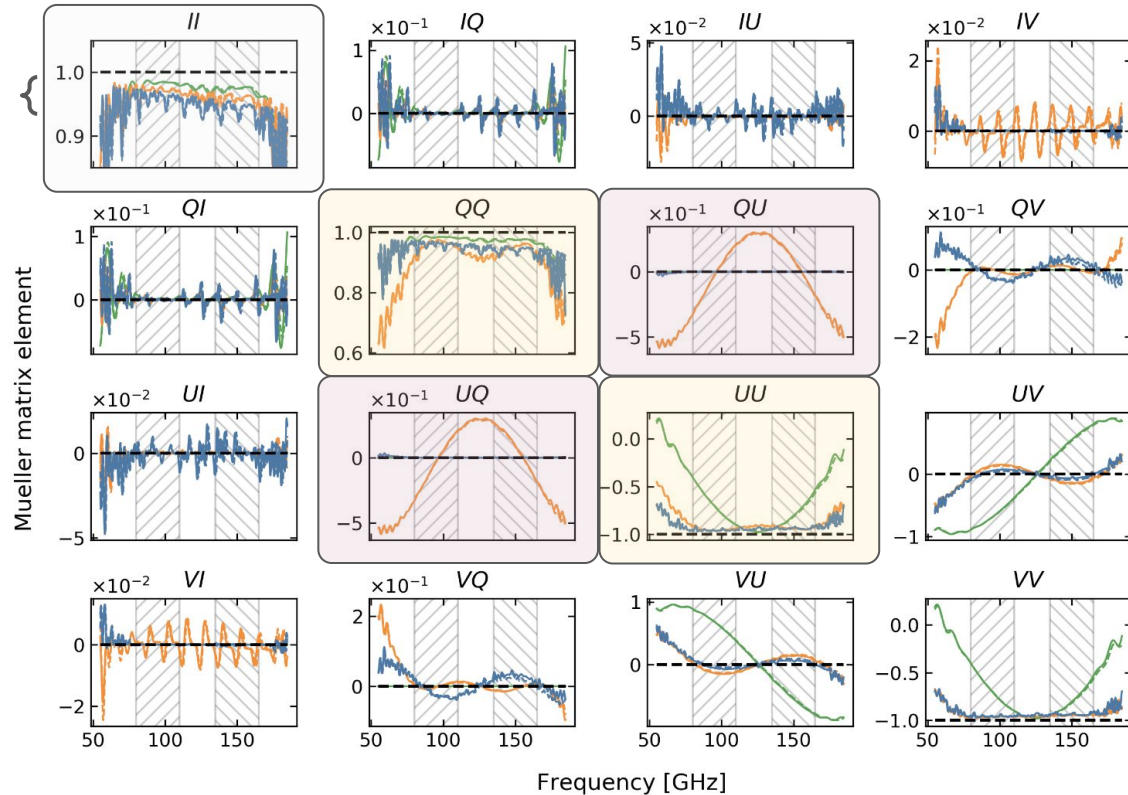
The telescope design defines the (frequency-dependent) far-field beam response of the instrument expressed as Stokes  $I, Q, U, V$  beams or equivalently as  $I, P, P^*, V$  beams

# HWP Mueller matrices

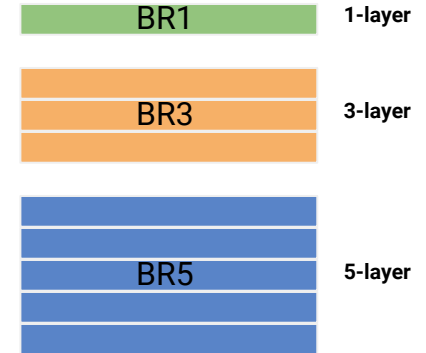
Overall sensitivity

Polarization modulation efficiency (QQ and UU)

Cross-polar leakage (QU/UQ)



Broadband (achromatic) polarization modulators obtained by stacking birefringent plates



— BR1  
 - - BR1 18°  
 — BR3  
 - - BR3 18°  
 — BR5  
 - - BR5 18°  
 - - Ideal

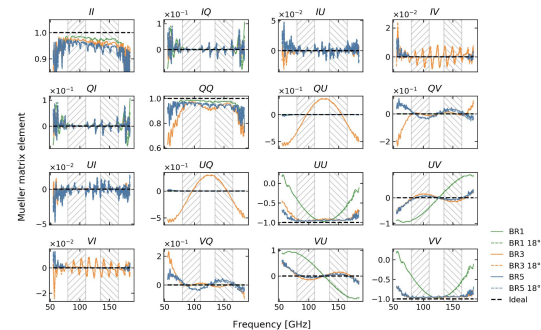
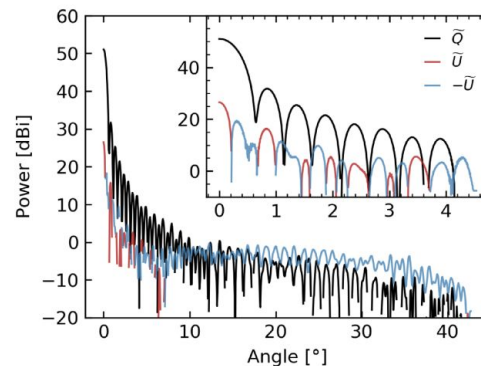
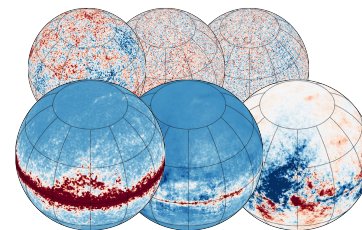
All configurations use the same 3-layer anti-reflection coating

Mueller matrices for arbitrary stacks calculated using T. Hileman's publicly available code: [https://github.com/tomessingerhileman/birefringent\\_transfer\\_matrix](https://github.com/tomessingerhileman/birefringent_transfer_matrix)



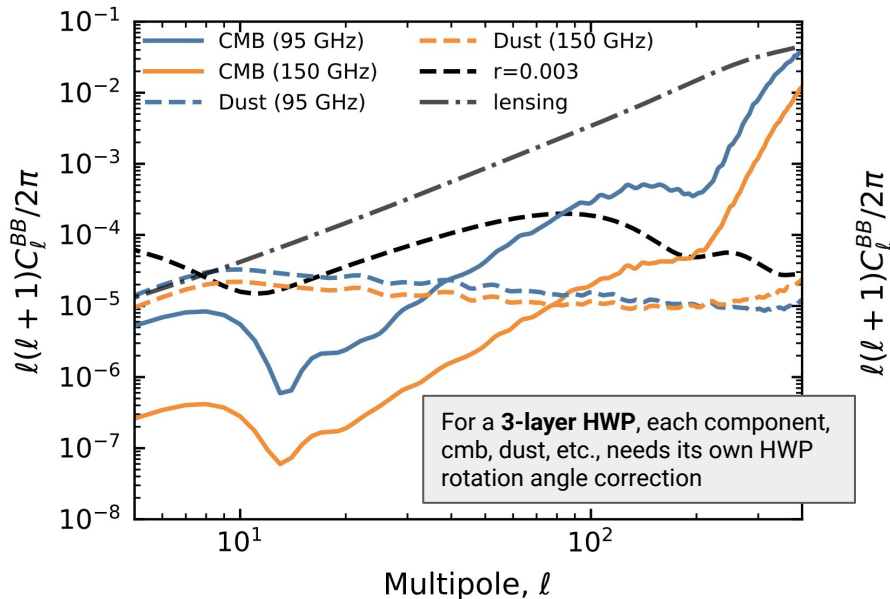
# The simulations

- We model 50 dichroic detectors sensitive to two 30-GHz-wide frequency windows centred at 95 and 150 GHz
- The detectors are evenly distributed on a square grid of a focal plane fed by a 30-cm aperture telescope
- In order to test frequency-dependent effects, we run simulations at seven sub-frequencies within a band (e.g. 80, 85, 90, 95, 100, 105, and 110 GHz for the 95-GHz band)
- Study the impact of different (PySM) foreground models and different HWP Mueller matrices while keeping everything else fixed

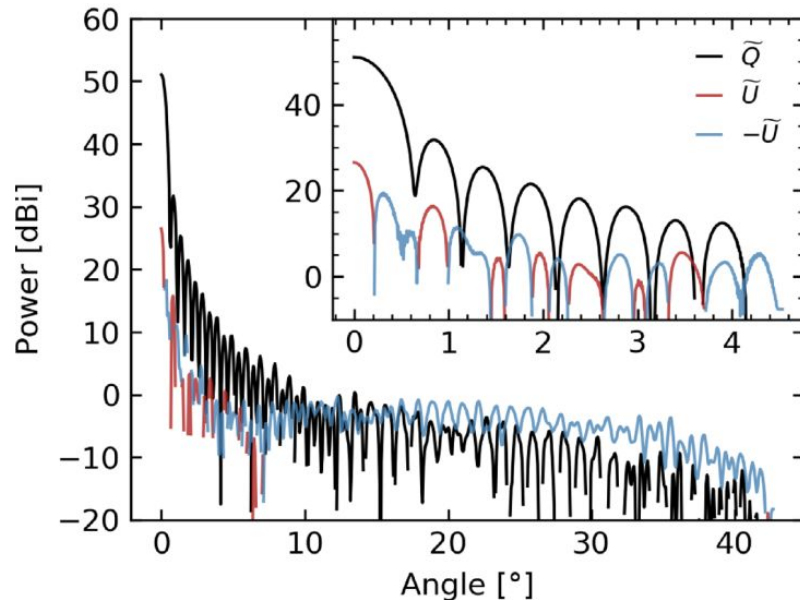


# Frequency-dependent phase angle

Incorrect phase angle correction: using phase angle for dust/CMB when observing CMB/dust



Residual from sidelobe coupling to Galaxv depends on HWP model



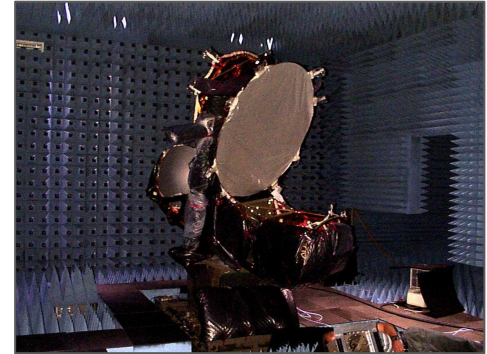
Map making will have to account for spectral energy distribution of sources; various foreground models impact  $B$ -mode residuals differently

# WMAP and *Planck* pre-flight characterization

Both characterized beam response using coherent measurement systems

**WMAP:** The Goddard Electromagnetic Anechoic Chamber (GEMAC) at Goddard Space Flight Center

**Summary from Lyman Page:** The measurements were really important for verifying that our models worked. **Understanding the optics was critical for mission success, and, we could not have understood them without being confident of the model as a function of frequency.**



GEMAC at  
Goddard  
Space Flight  
Center



Roof of  
Jadwin Hall  
(Princeton  
physics dept.)

# WMAP and *Planck* pre-flight characterization

Both characterized beam response using coherent measurement systems

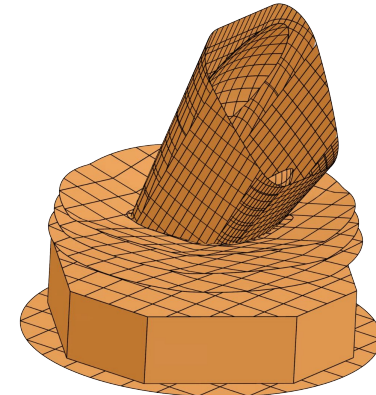
## ***Planck***: CATR at Thales Alenia Space

RF Qualification Model at four frequencies: 30, 70, 100, and 320 GHz. Dynamic range of the measurement was better than 90 dB for 30 GHz, 100 dB at 70 and 100 GHz, and 90 dB at 320 GHz.

Although in principle the mechanical setup allowed measurements of the full  $4\pi$  steradians area, time-wise this was not practical.



CATR setup at Thales Alenia Space



GRASP model of Planck optics

# Planck lessons learned

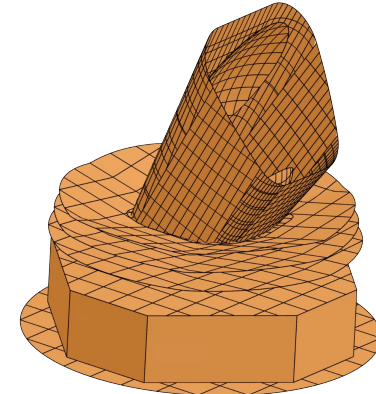
Compact Antenna Test Range (CATR) measurements at Thales Alenia Space allowed us to verify and refine our GRASP physical optics (PO) models of the telescope.

## **This model was critical for the mission:**

- a) It provided a prior that informed all beam analysis (both LFI and HFI)
- b) It was used for LFI cosmological analysis (see e.g., Planck 2013 results. V. LFI calibration)
- c) Model not fully consistent with HFI beam reconstruction measurements, instead HFI analysis beams based on Jupiter, Saturn, and Mars observations



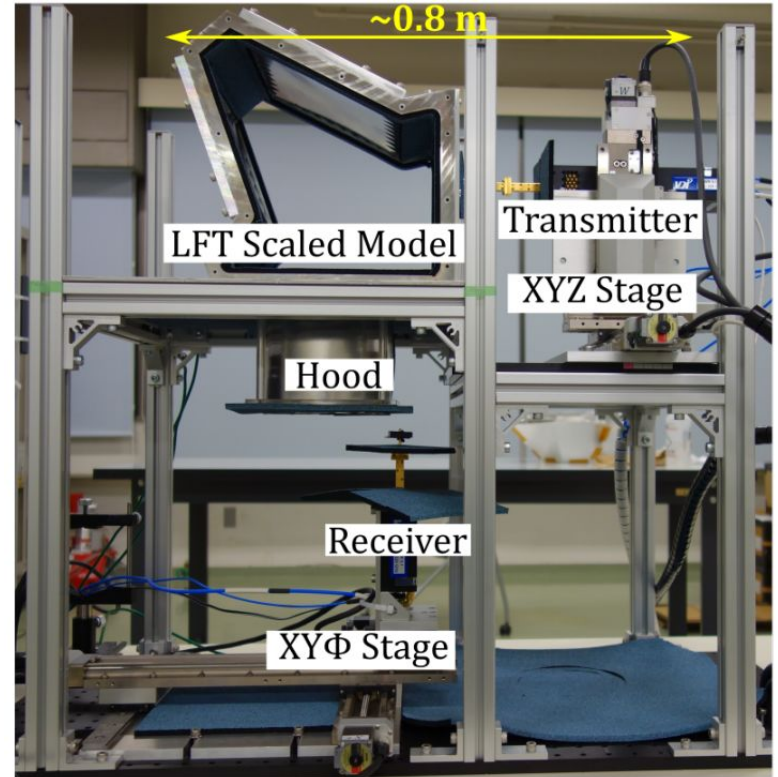
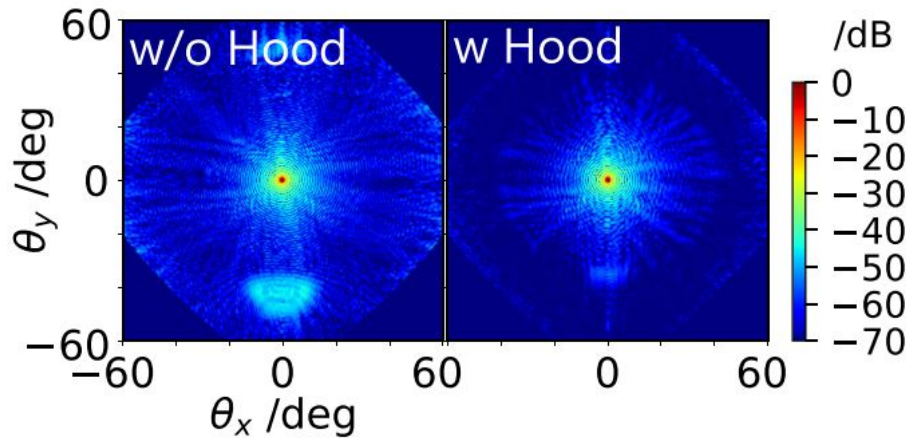
CATR setup at Thales Alenia Space



GRASP model of Planck optics

# Advanced calibration efforts 1/2

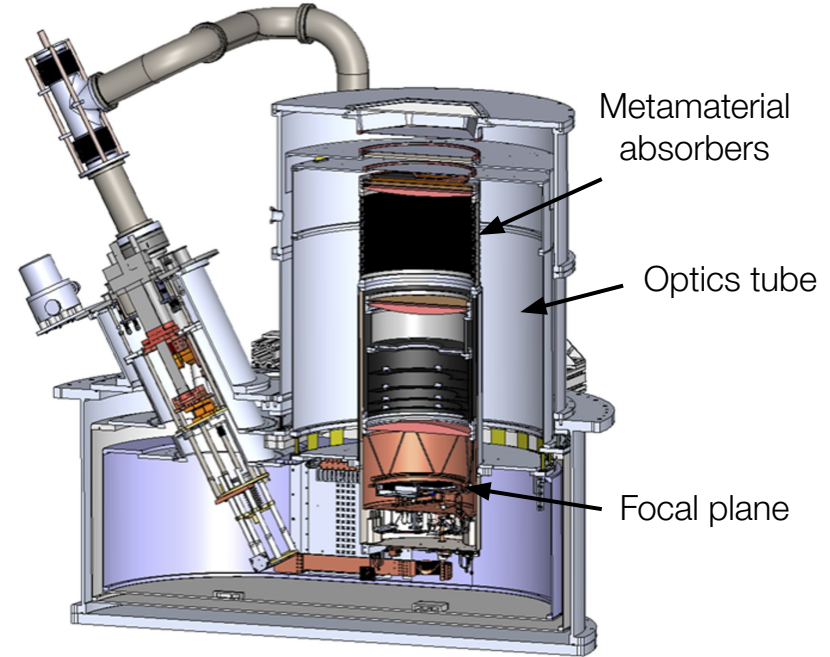
- Testing of a 1:4 scaled version of the LiteBIRD low-frequency telescope (140-220 GHz) at the Univ. of Tokyo (Takakura, Sekimoto, et al., 2019)



Credit: Hayato Takakura

# Advanced calibration efforts 2/2

- Testing of reimaging optics tubes for the Simons Observatory Large Aperture Telescope at U. Chicago (Chesmore, McMahon, et al., in preparation)
- **Goal:** Characterize and mitigate systematics prior to deployment in the SO LAT 13-tube cryogenic receiver
- Measurements conducted with optical components at 4 and 40 Kelvin

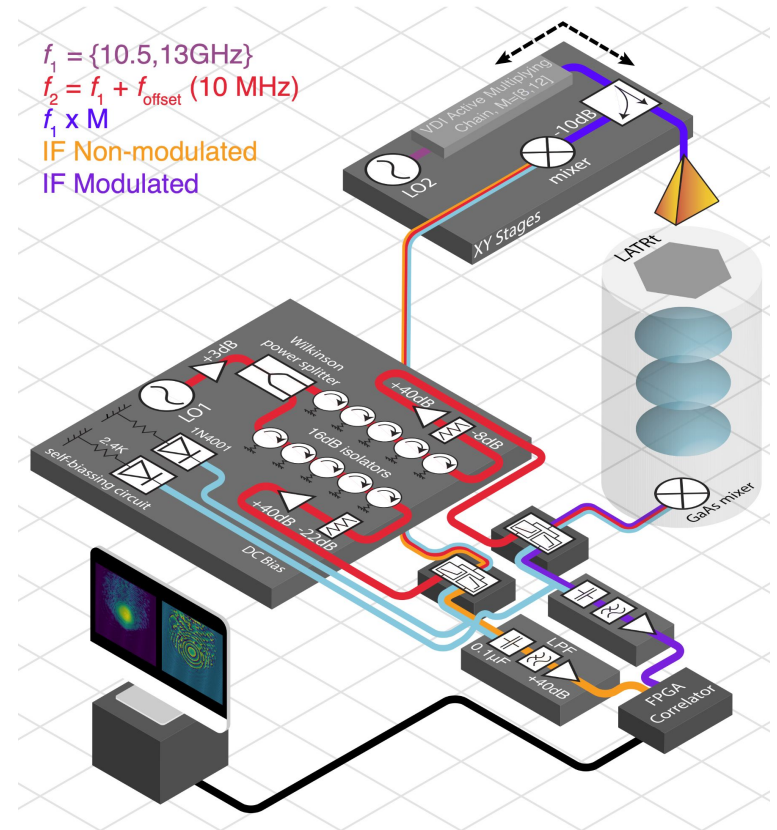
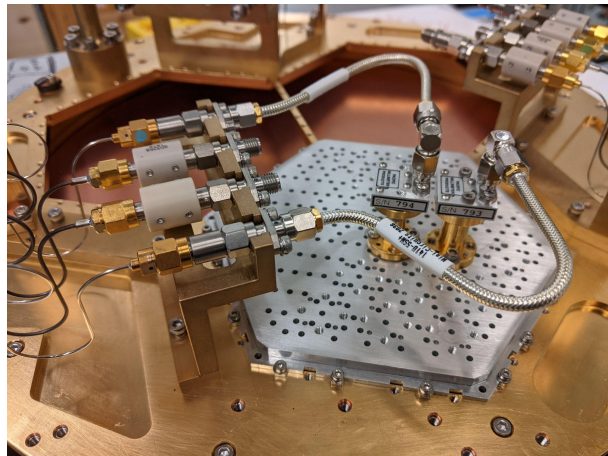
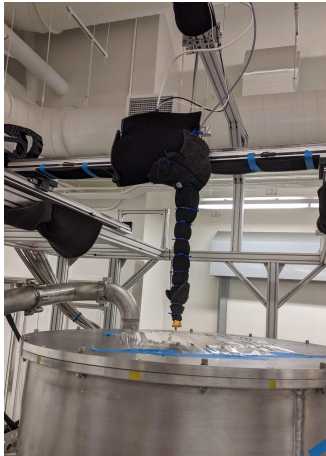


The Simons Observatory Small Aperture Telescope Cryostat

*Credit: Grace Chesmore*

# Advanced calibration efforts 2/2

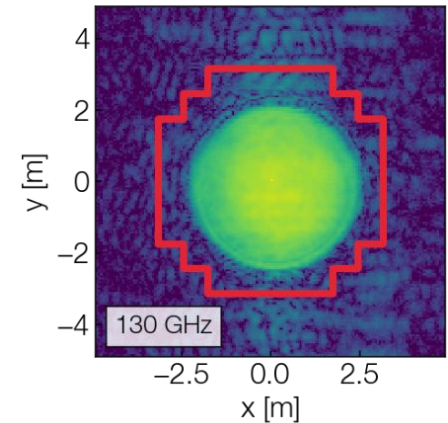
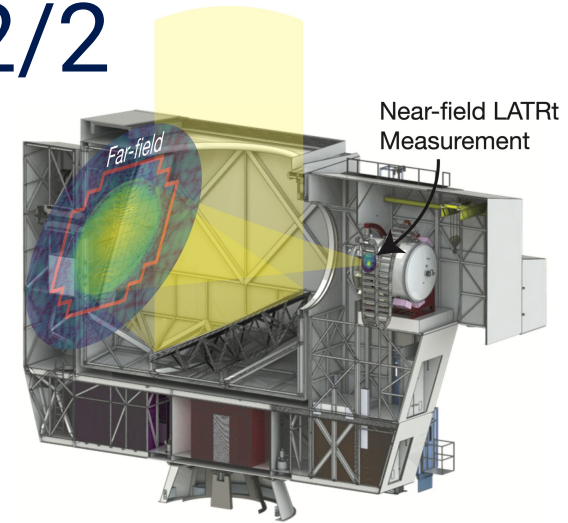
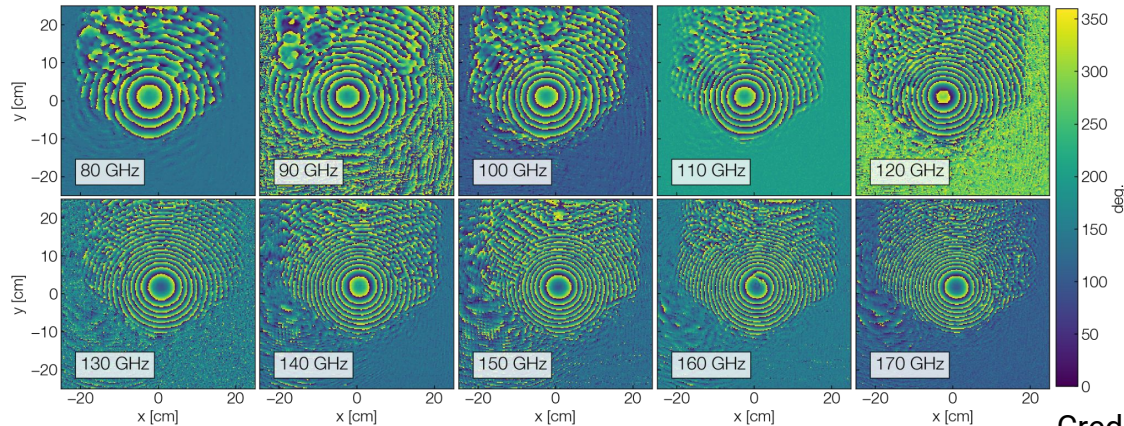
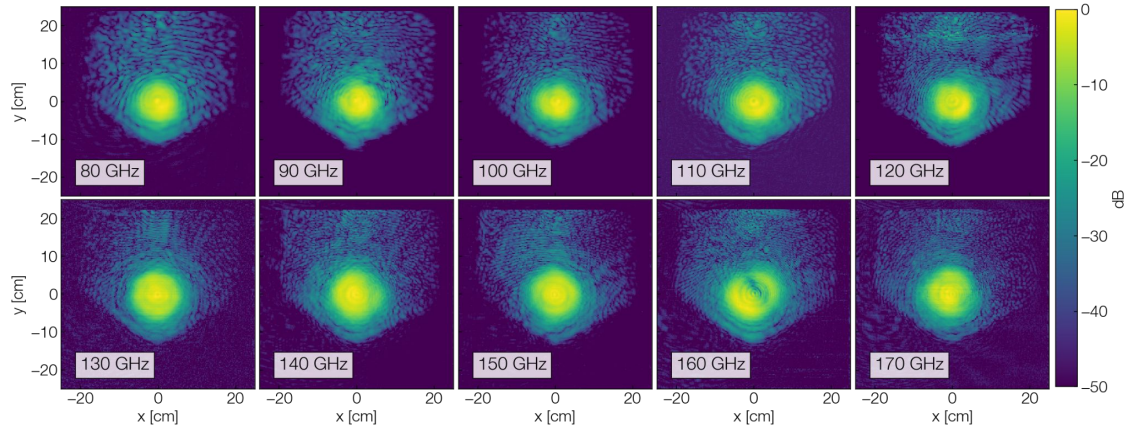
- Testing of reimaging optics tubes for the Simons Observatory Large Aperture Telescope at U. Chicago (Chesmore, McMahon, et al., in preparation)



Credit: Grace Chesmore



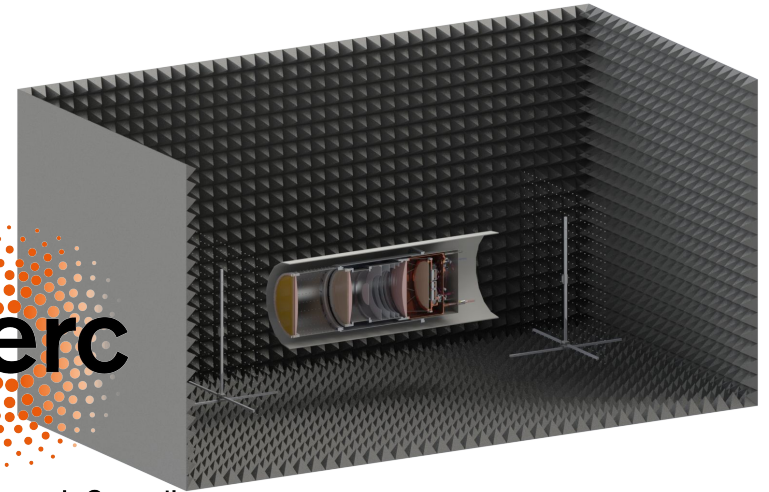
# Advanced calibration efforts 2/2



Credit: Grace Chesmore

# ERC-funded CMBeam project starting '22

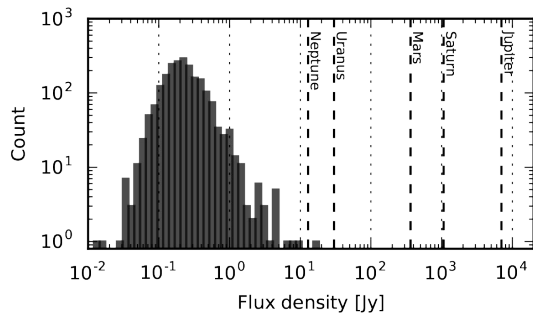
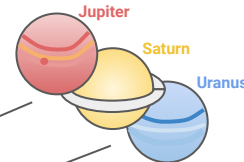
- **Primary objective:** Advance cryogenic holography (phase-sensitive near field beam mapping) measurement techniques performed in the 40-400 GHz range and contribute to studies of optical systematics for current and next-generation CMB experiments
  - Build a prototype/qualification optics tube that is representative of current-gen experiment and calibrate extensively in the lab
- First 3-year postdoc position announced (contact me for details)



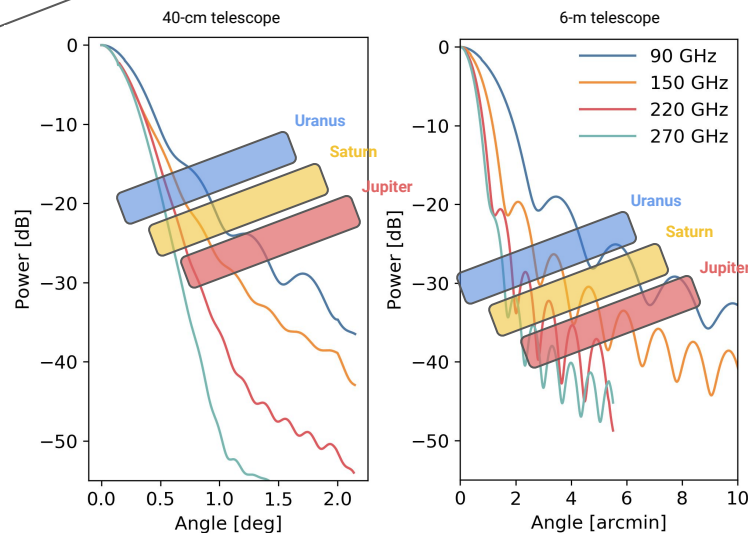
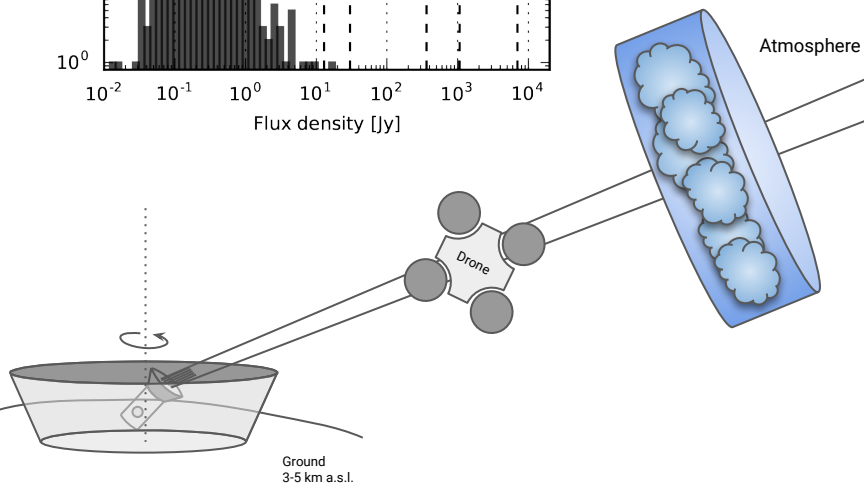
European Research Council

Established by the European Commission

# Point source observations



Caption: Flux density at 217 GHz (1.38 mm) for all point sources seen by the Planck satellite  
**The planets are by far the brightest mm-wave sources on the sky**

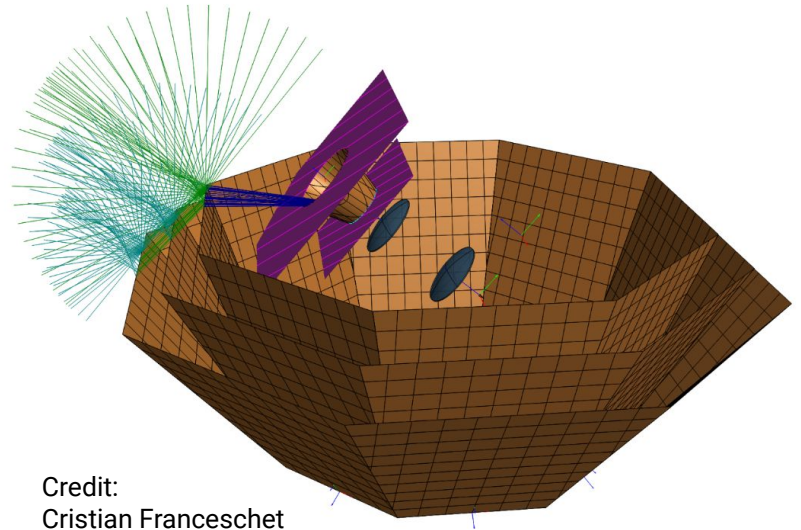


Azimuthal beam profiles,  $B(\theta)$ , for 40-cm and 6-m diameter ground-based telescopes.

$$\text{signal} \propto \int B(\theta - \theta_0, \phi - \phi_0) P(\theta, \phi) d\Omega$$

# Where do our modeling capabilities fall short and what can we do about it?

- Optical modeling relies on proprietary software (GRASP, HFSS, Zemax, etc) with little to no support for distributed computing
- We don't know how to efficiently model diffraction effects on radiation shields, large ground screens, etc.
- Thermal and mechanical modeling of large-diameter filters and shaders critical for next-generation satellite experiment
- Lenses with metamaterial anti-reflection coatings, broadband absorbers, reflective focal planes, filter simulations of these complex optical systems that are not yet computationally feasible
- Detector/feedhorn optimization and telescope optimization is currently decoupled



Credit:  
Cristian Franceschet

[Framework for analysis of next generation, polarised CMB data sets in the presence of galactic foregrounds and systematic effects – Vergès et al. \(2020\)](#)

[The Simons Observatory: Bandpass and polarization-angle calibration requirements for B-mode searches – Abitbol et al. \(2020\)](#)

[New Extraction of the Cosmic Birefringence from the Planck 2018 Polarization Data – Minami and Komatsu \(2020\)](#)

[A new limit on CMB circular polarization from SPIDER – Nagy et al \(2016\)](#)

[Spin characterisation of systematics in CMB surveys – a comprehensive formalism – McCallum, Thomas, Brown, Tessore \(2020\)](#)

From [BeyondPlanck I. Global Bayesian analysis of the Planck Low Frequency Instrument data](#), Section 1.4:

*Indeed, only toward the end of the Planck mission period did it become evident that the **single most limiting factor for the overall analysis was neither instrumental systematics nor astrophysical foregrounds as such, but rather the interplay between the two.** Intuitively speaking, the problem may be summarized as follows: One cannot robustly characterize the astrophysical sky without knowing the properties of the instrument, and one cannot characterize the instrument without knowing the properties of the astrophysical sky. The calibration and component separation procedures are intimately tied together.*

[BICEP / Keck Array XII: Constraints on axion-like polarization oscillations in the cosmic microwave background – BICEP/Keck Array collaboration \(2020\)](#)

[Instrumental systematics biases in CMB lensing reconstruction: a simulation-based assessment – Mirmelstein, Fabbia, Lewis, and Peloton \(2020\)](#)

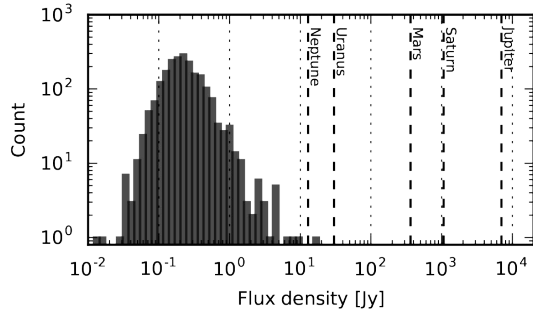
[Planck intermediate results. XLVI. Reduction of large-scale systematic effects in HFI polarization maps and estimation of the reionization optical depth – Planck Collaboration \(2016\)](#)

[Two-year Cosmology Large Angular Scale Surveyor \(CLASS\) Observations: A Measurement of Circular Polarization at 40 GHz – Padilla et al. \(2019\)](#)

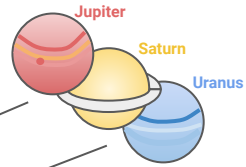
[The Atacama Cosmology Telescope: Constraints on Cosmic Birefringence – Namikawa et al. \(2020\)](#)

# Backup

# Point source observations

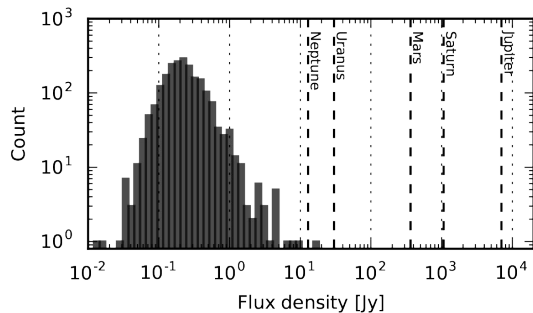
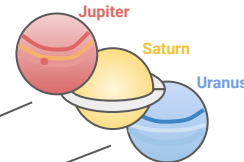


Caption: Flux density at 217 GHz (1.38 mm) for all point sources seen by the Planck satellite  
**The planets are by far the brightest mm-wave sources on the sky**

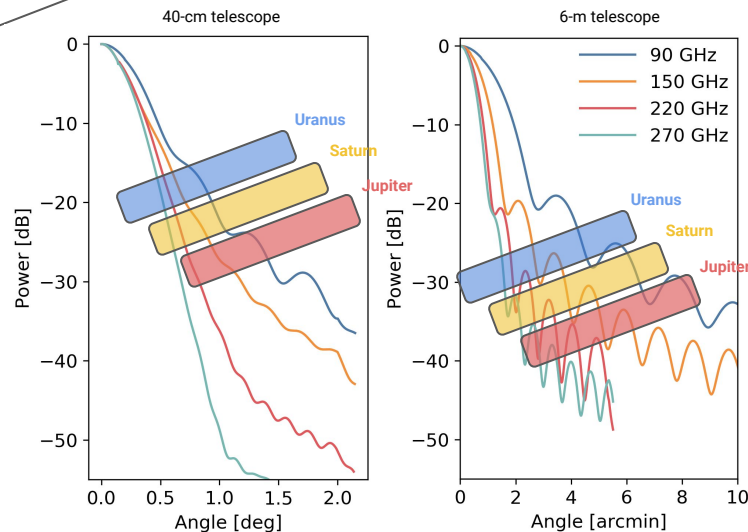
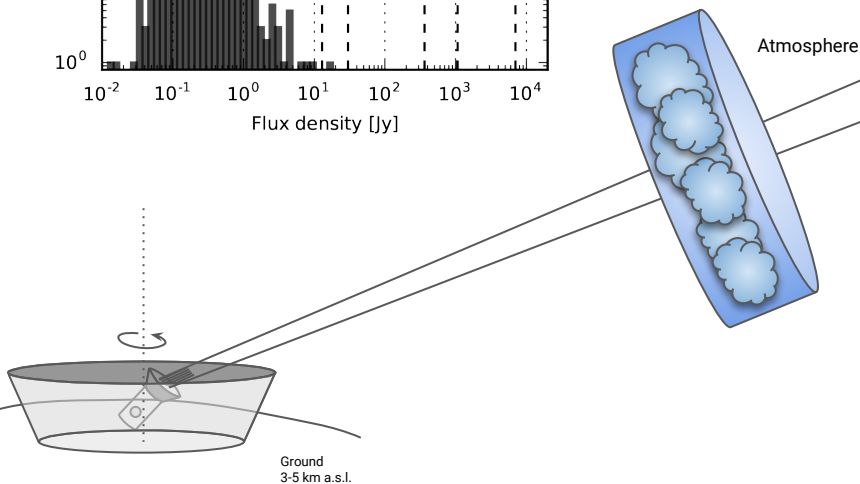


$$\text{signal} \propto \int B(\theta - \theta_0, \phi - \phi_0) P(\theta, \phi) d\Omega$$

# Point source observations



Caption: Flux density at 217 GHz (1.38 mm) for all point sources seen by the Planck satellite  
**The planets are by far the brightest mm-wave sources on the sky**



Azimuthal beam profiles,  $B(\theta)$ , for 40-cm and 6-m diameter ground-based telescopes.

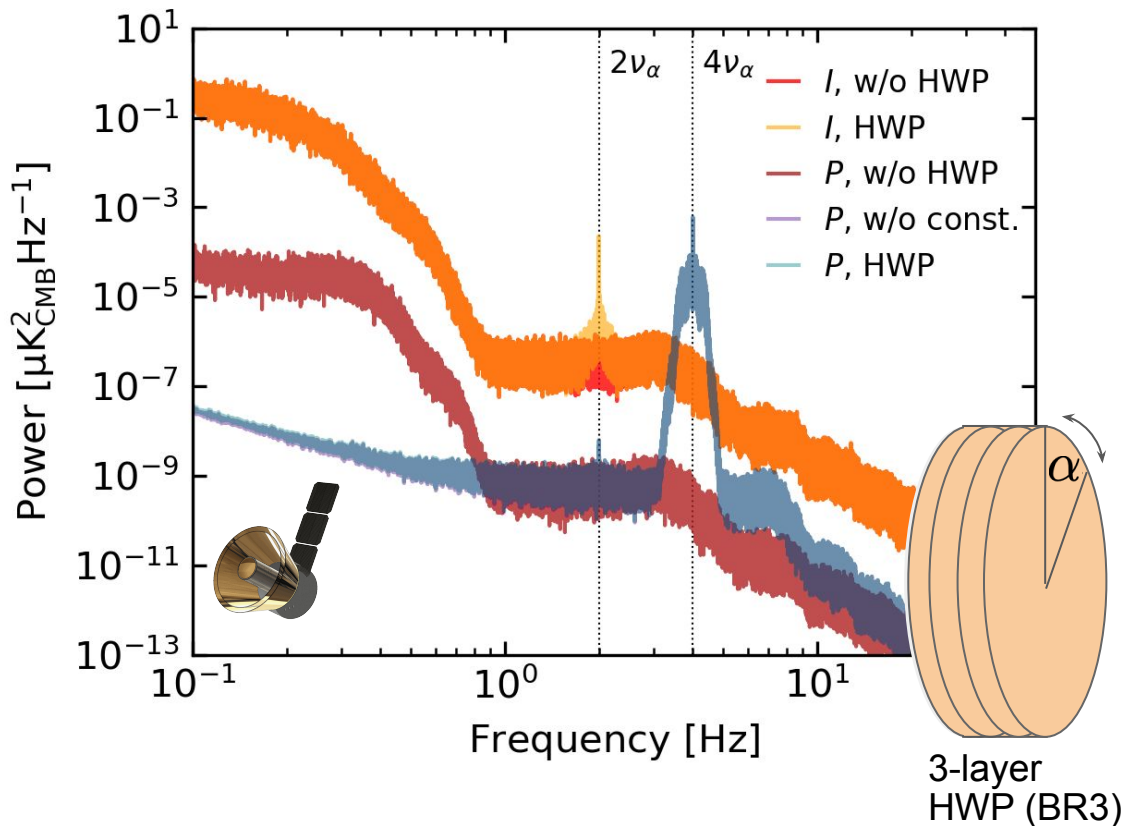
$$\text{signal} \propto \int B(\theta - \theta_0, \phi - \phi_0) P(\theta, \phi) d\Omega$$



# Forward-modeling misconceptions

- Simulation of 400 detectors scanning the entire sky for 365 days at 96.7 Hz producing  $1.2 \times 10^{12}$  samples takes  $\mathcal{O}(10)$  hours on a 4-socket 16-core Intel Xeon E7-4850 (2.1 GHz) node with 512 GB of RAM
  - Band-limited beam convolution up to  $\ell_{\max} = 700$  and  $m_{\max} = 4$ .
  - Stokes  $I, Q, U$ , (and even  $V$ ) beams scanning of input Stokes  $I, Q, U, (V)$  maps
- Full-mission (3-years and 3000 channels) full-sky beam convolution simulations are certainly realistic with current technology
  - Would take 7 days per realization with the above architecture

# Signal PSD for 2 hours of 3-layer HWP



## Ideal HWP

- $Q, U$  modulated by  $4\nu_\alpha$
- $I, V$  unmodulated

Non-ideal HWP gives additional terms:

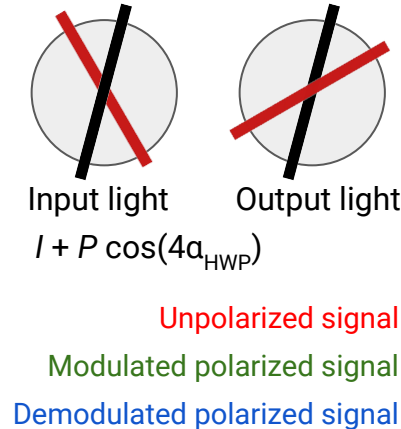
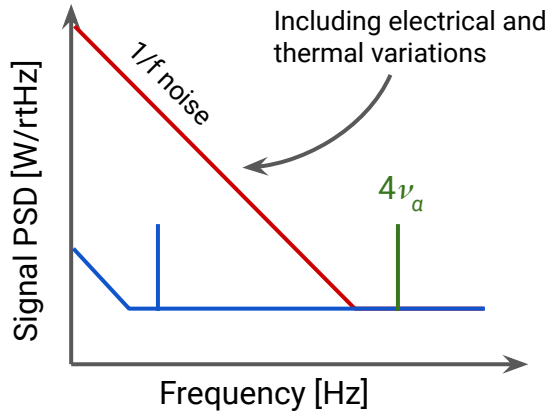
- $Q, U$  mixed by effective offset in  $\alpha$
- $Q, U$  modulated by  $2\nu_\alpha$
- $Q, U$  unmodulated
- $I, V$  modulated by  $2\nu_\alpha$

# Half-wave plate

## Operating Principle

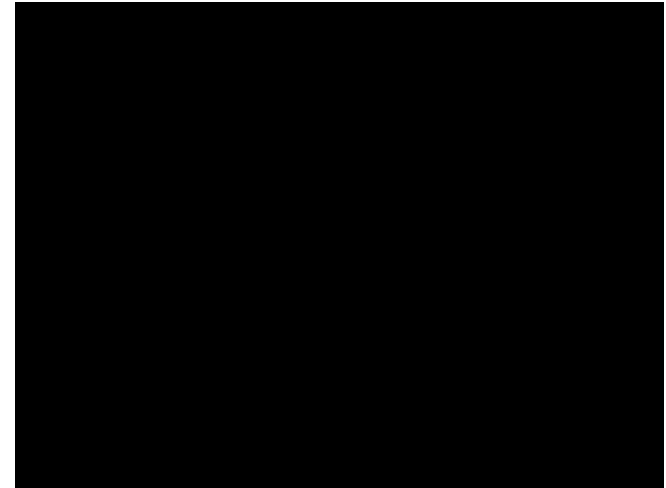
- A rotating birefringent plate modulates polarization at  $4\nu_\alpha$
- The first sky-side optical element

— Pol angle  
— HWP axis



See wide array of LiteBIRD SPIE 2020 papers, including:

- Y. Sakurai et al: <https://arxiv.org/abs/2101.06342>
- K. Komatsu et al: <https://arxiv.org/abs/1905.13520>
- L. Montier et al: <https://arxiv.org/abs/2102.00809>



Rotation test of superconducting magnetic bearing system in the 4K cryostat. Stable rotation at cryogenic temperature ( $< 10\text{K}$ ).

# Outline from Ludo

Your expertise and contribution will be important additions to our workshop. Hence we are pleased to invite you to give a talk on the specific subject of “**Criticality of beam knowledge for polarization and distortion measurements**”, which will serve to introduce the session on “Polarised Beam modelling challenges”.

We hope your talk will focus, on the one hand, on the impact of uncertainties related to the optical response on the analysis of CMB data (anisotropies, spectral distortions). **How can the knowledge of the beam be parametrized, how can we propagate these parameters through the analysis chain, and how can we relate the results to the inputs? Are there generic lessons from past experiments?** What are plans for experiments in development? **On the other hand, your talk should also discuss how we can quantify our knowledge of the optical response, based on measurement and modelling, in both test environments and experiment operations. What are realistic achievable levels in different experimental settings?**

# Knowing your beams

**Abstract:** The cosmic microwave background (CMB) has played a foundational role in the establishment of the standard model of cosmology. Driven by significant technological advances, future CMB experiments aim to make dramatic strides in our understanding of the universe. Some of our most ambitious efforts, however, run the risk of being hamstrung by poorly-understood instrument effects, systematics. A commonly-discussed class of systematic effects relate to our optical systems in one way or another. In this talk, I will review some of the challenges that past CMB missions have faced and highlight lessons learned. I will present algorithms that have been developed to help us understand the impact of optical non-idealities and summarize key results from the applications of those. I will conclude by reviewing some of the challenging calibration requirements for upcoming missions and discuss how the community can work towards meeting those.

# Holography

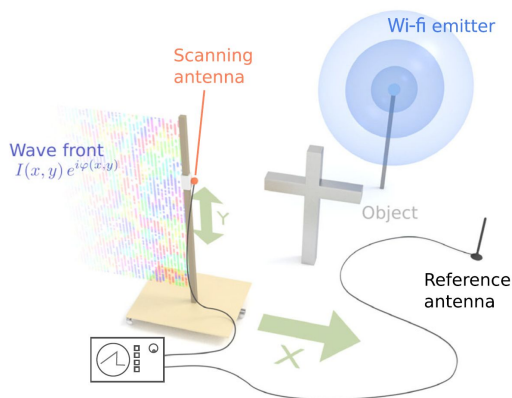
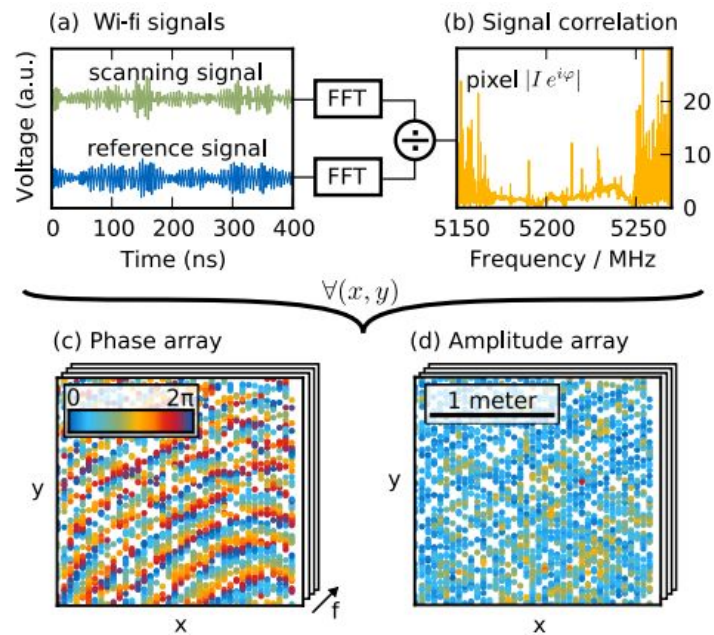
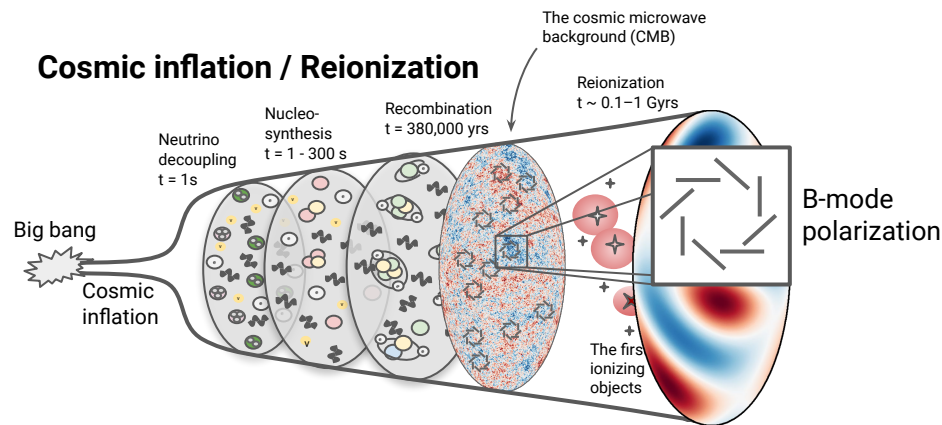


FIG. 1. Experimental setup. Stray radiation from a commercial router is employed to image meter-sized objects (gray cross) by digital holography. We record a hologram of wi-fi radiation by a synthetic aperture approach. A wi-fi antenna (scanning antenna) is moved across a 3 by 2 meter plane, pointwise registering wi-fi signals. The signal phase is recovered by a homodyne scheme, normalizing the signals to the signal of a stationary antenna (reference antenna).



Credit: Holl & Reinhardt, PRL (2017)

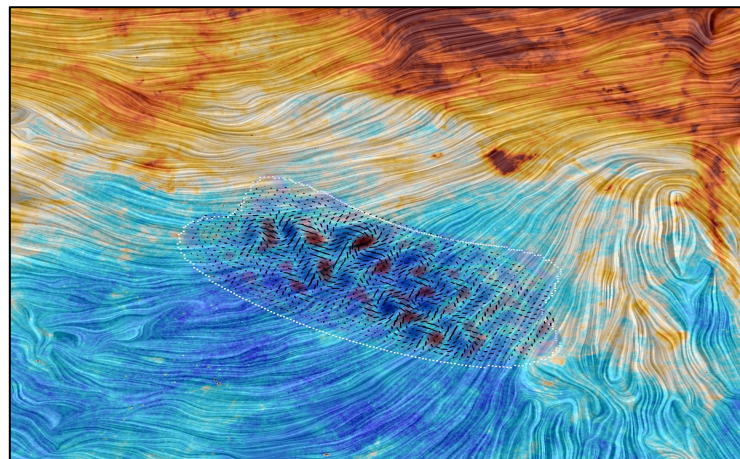
# Scientific motivation



When did reionization occur?  $\rightarrow$  optical depth ( $\tau$ )  
What were the main ionizing sources?

Reionization leaves an imprint in CMB polarization on very large angular scales

We have the technology to make a definitive search for a signal from reionization and cosmic inflation in CMB polarization maps

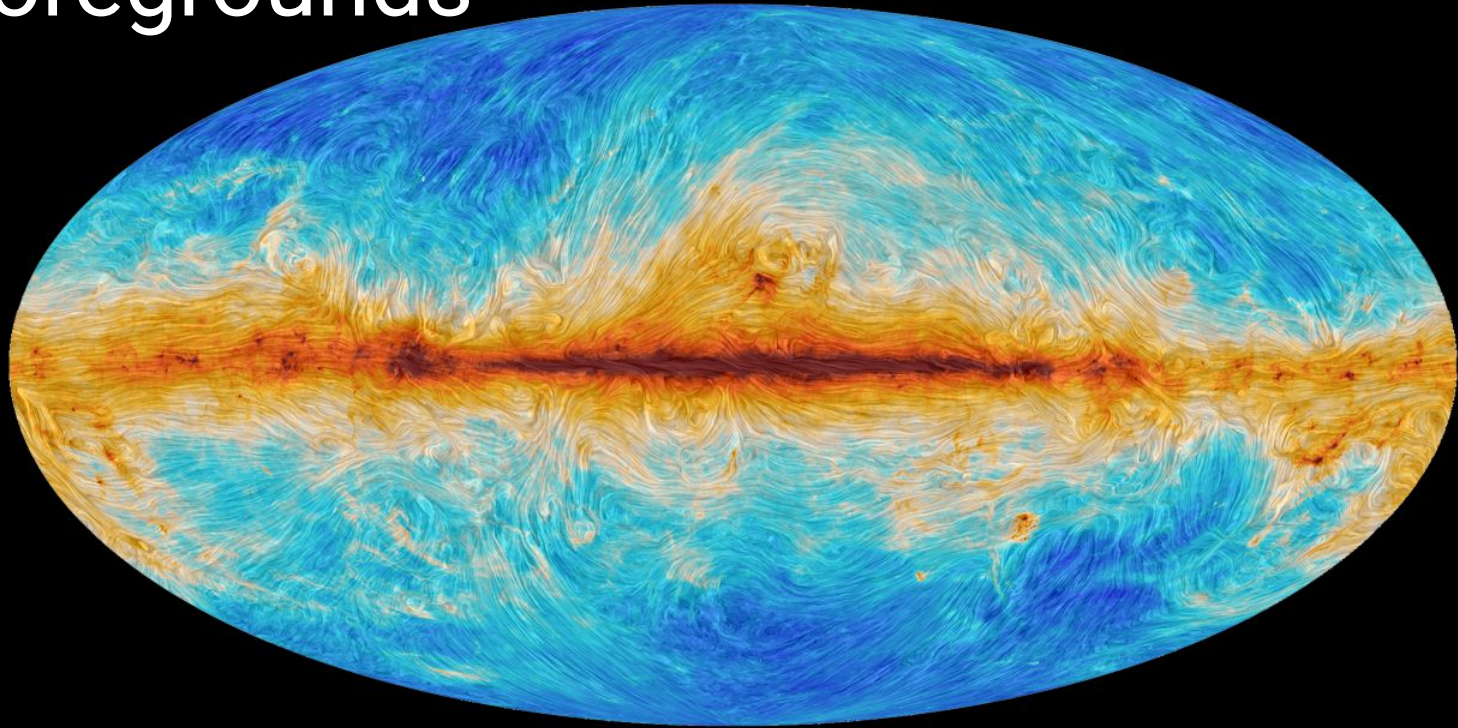


Composite Planck and BICEP2/Keck map

Two key challenges:

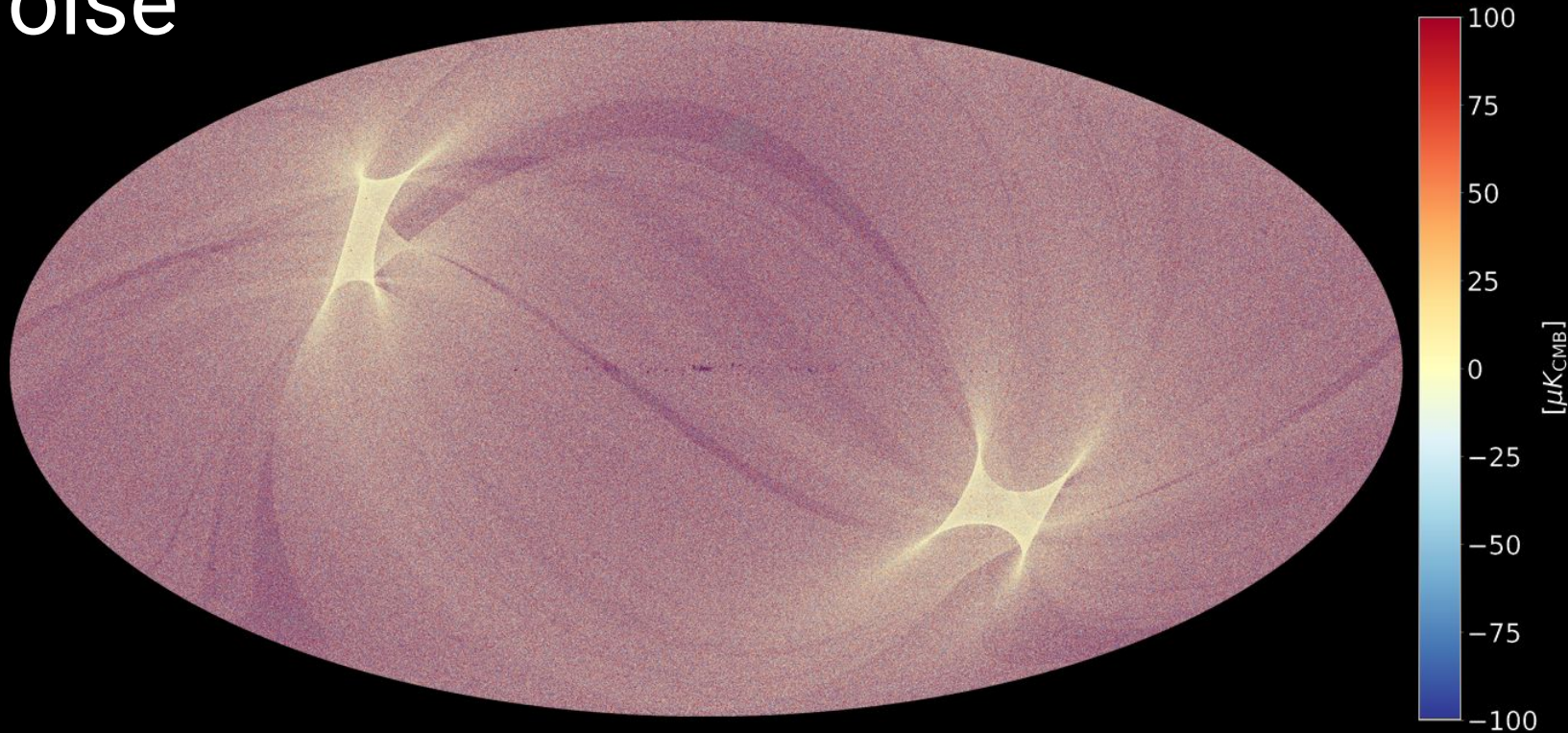
- Galactic foregrounds (above)
- **Optical systematics**

# 1 Foregrounds

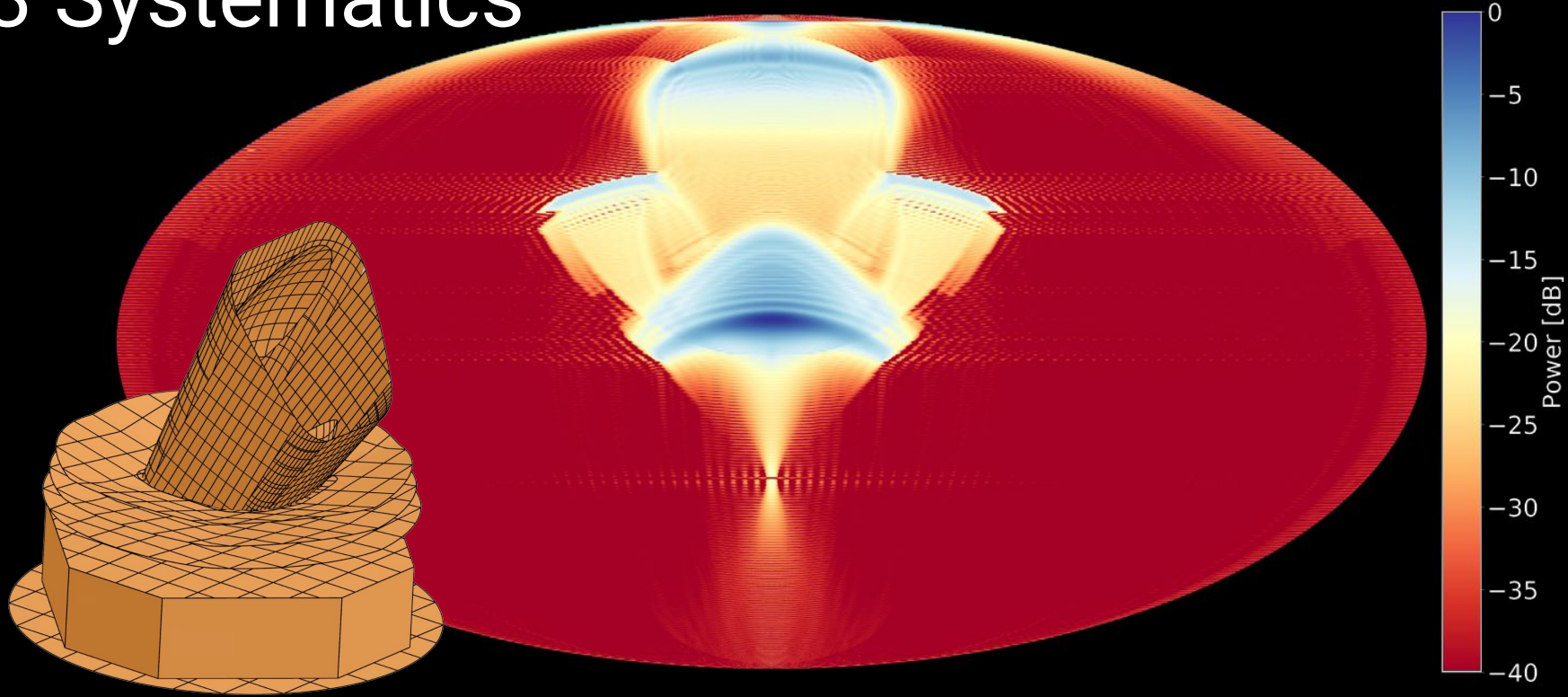




# 2 Noise



# 3 Systematics



Planck LFI 44 GHz sidelobe map

# Maps and spectra

These maps are described with spherical harmonic functions

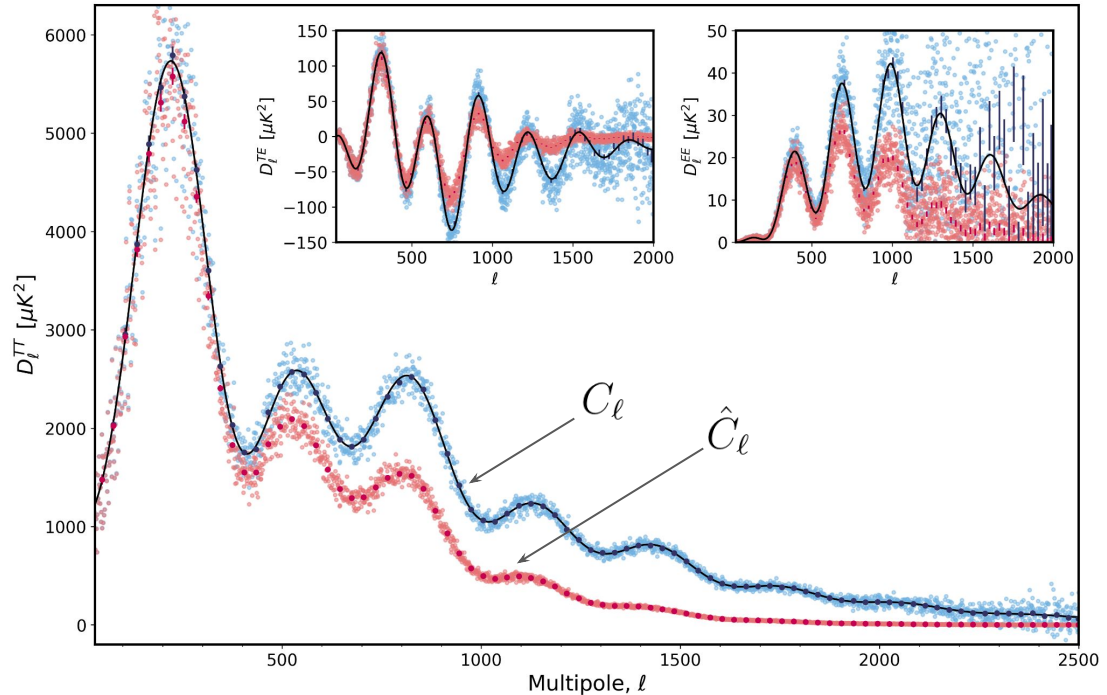
$$M(\theta, \phi) = \sum_{\ell=0}^{\infty} \sum_{m=-\ell}^{\ell} a_{\ell m} Y_{\ell m}(\theta, \phi)$$

The  $a_{\ell m}$  coefficients are then used to calculate an angular power spectrum

$$\hat{C}_{\ell} = \frac{1}{2\ell + 1} \sum_{m=-\ell}^{\ell} |a_{\ell m}|^2$$

The telescope has finite resolution, described by the beam function,  $B(\theta, \phi)$ , and the angular power spectrum that we calculate from our maps is biased; a correction needs to be applied

$$\hat{C}_{\ell} = C_{\ell} b_{\ell}^2 \quad \text{where} \quad b_{\ell} = \int d\Omega B(\theta, \phi) Y_{\ell 0}(\theta, \phi)$$



# Beam modeling challenges

Unfortunately, this beam correction can fail for a multitude of reasons

We do not know our  $B(\theta, \phi)$

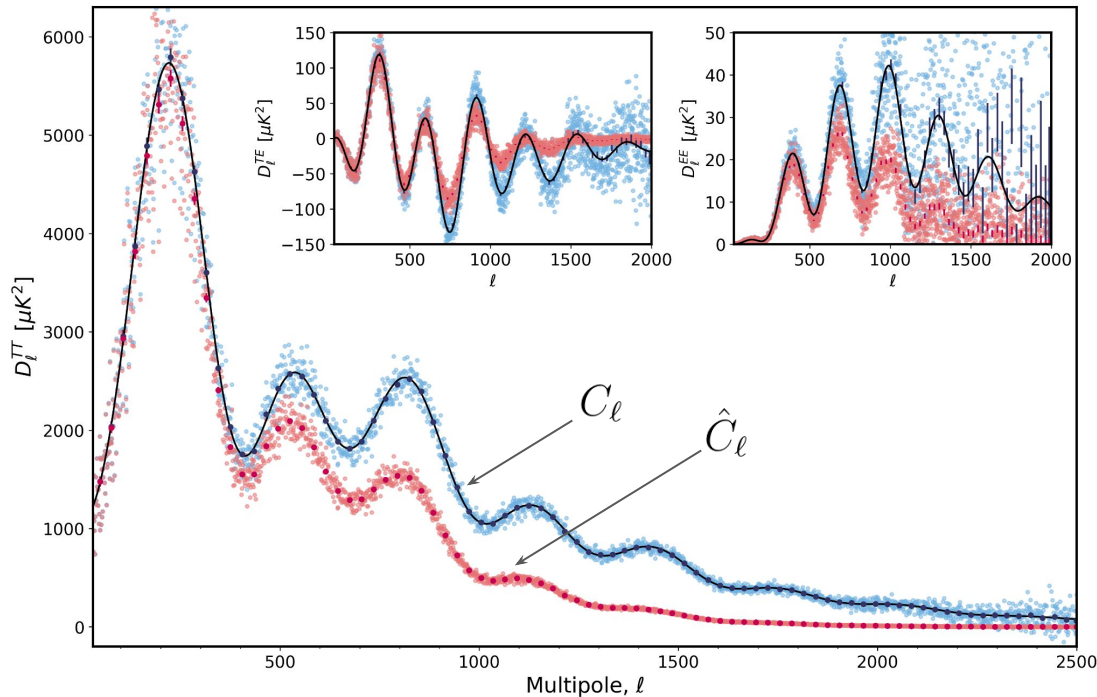
The beam is not azimuthally symmetric

- Scan strategy matters
- Need for time-domain sims

Beams are extended (cover  $4\pi$  srad)

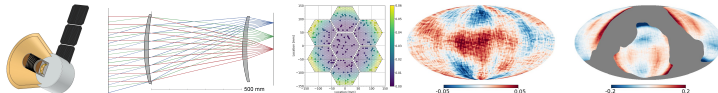
- Signal that we attribute to pixels in our map can come from spurious beam sidelobe coupling to the Galaxy

The very faint and polarized signal that we are studying forces us to understand polarization angle and efficiencies incredibly well



# beamconv published in 2018

- Open source spherical harmonic beam convolution algorithm **written in Python**
  - <https://github.com/AdriJD/beamconv>
- Spin-spherical harmonic representations of the (polarized) beam response and sky to generate simulated CMB detector signal timelines
- **Beams can be arbitrarily shaped; pointing timelines can be read in or calculated on the fly;** optionally, the results can be binned on the sphere
- First paper: Duivenvoorden, JEG, and Rahlin, MNRAS (2018) ([arXiv:1809.05034](https://arxiv.org/abs/1809.05034))
  - Core algorithm first described in Prézeau and Reinecke, ApJS, 190:267–274 (2010)



A. Duivenvoorden  
Stockholm  
University '19

